BILINGUAL PUBLISHING GROUP

Research in Ecology

https://journals.bilpubgroup.com/index.php/re

ARTICLE

Environmental Drivers and Group Defense Strategies in Diffusive and Non-Diffusive Predator-Prey Dynamics

Muhammad Shoaib Arif [1*] **, *Asad Ejaz*** [2]

[1] *Department of Mathematics and Sciences, College of Sciences and Humanities, Prince Sultan University, Riyadh 11586, Saudi Arabia*

[2] *Department of Mathematics, Air University, Islamabad 44000, Pakistan; asadijaz64@yahoo.com*

ABSTRACT

Predator-prey dynamics are strongly influenced by environmental factors, such as the availability of resources, habitat quality and climatic conditions, which determine species survival, species reproduction and aggregate defensive behaviour. Using these ecological processes, a three-species predator-prey model is formulated and analysed, with prey group defence dependent on an environmental logistic function. Predation intensity, influenced by environmental conditions, is examined, and the long-term dynamics of interacting populations under these conditions are explored. Biologically plausible equilibrium points are verified, and their local and global stability is thoroughly investigated by the Routh-Hurwitz criterion and Lyapunov function methods, respectively. The governing equations are modified to include diffusion terms to describe the dispersal of species in space, leading to a reaction-diffusion system that describes the spread of species in heterogeneous habitats. A three-level finite difference scheme is developed to approximate the diffusive model, and its numerical stability is examined through Von Neumann analysis. Furthermore, the stability of the reaction-diffusion system is investigated using a Fourier series expansion and the Routh-Hurwitz criterion. Increased effective predation, larger population oscillations, and less stable coexistence between species are shown to result from a reduction in the strength of environmentally regulated group defence. In contrast, diffusion can help smooth spatial population gradients, making the ecosystem more resilient to effective predation and promoting species redistribution. The mathematical model

*CORRESPONDING AUTHOR:

Muhammad Shoaib Arif, Department of Mathematics and Sciences, College of Sciences and Humanities, Prince Sultan University, Riyadh 11586, Saudi Arabia; Email: marif@psu.edu.sa

ARTICLE INFO

Received: 18 June 2026 | Revised: 30 July 2026 | Accepted: 18 August 2026 | Published Online: 17 September 2026
DOI: https://doi.org/10.30564/re.v8i5.13667

CITATION

Arif, M.S., Ejaz, A., 2026. Environmental Drivers and Group Defense Strategies in Diffusive and Non-Diffusive Predator-Prey Dynamics. Research in Ecology. 8(5): 71–104. DOI: https://doi.org/10.30564/re.v8i5.13667

COPYRIGHT

Copyright © 2026 by the author(s). Published by Bilingual Publishing Group. This is an open access article under the Creative Commons Attribution-NonCommercial 4.0 International (CC BY-NC 4.0) License (https://creativecommons.org/licenses/by-nc/4.0/).

proposed here can contribute to a better understanding of the complex interplay between environmental drivers, collective defense, and spatial dispersion in predator-prey dynamics and is potentially applicable to ecological modelling, biodiversity conservation, habitat management, and the analysis of spatially structured ecosystems.

Keywords: Group Defense; Stability; Bifurcation; Routh-Hurwitz Criterion; Lyapunov Function; Explicit Numerical Scheme

1. Introduction

Predator/prey dynamics in complex ecological systems have always been of interest to scientists and ecologists. The interactions of these species determine the basic structure of life on Earth and play a key role in the stability and resilience of the ecosystem. Ecological predator-prey models have gradually shed light on the dynamics behind the rise and fall of species populations by providing a needed perspective on the functioning of these complex relationships. While there are several models, no one has yet explained how prey species, which are normally helpless and vulnerable, can endure the constant attacks of predators.

This study explores the central issue of the ecological dilemma by focusing on the enigmatic nature of Factor-Guided Group Defense Mechanisms in predator-prey models with both diffusive and non-diffusive dynamics. Understanding the processes that underlie prey defence strategies and how they may change under different environmental conditions has broad implications for the conservation and management of natural ecosystems. This work not only enriches theoretical knowledge of ecological processes but also deepens understanding of the complex methods required to navigate the dangerous realm of predation and highlights nature's fragile balance amid persistent challenges.

Oscillatory systems of differential equations are commonly observed in a wide range of ecological models and the field of mathematical biology[1]. Relaxation oscillators are a class of oscillators characterised by two distinct time scales. If the time scale of the activator is significantly shorter, several activator-inhibitor models exhibit this characteristic[2]. A defining feature of relaxation oscillators is the phenomenon known as the excitation cycle[3]. This limit cycle can be eliminated via homoclinic bifurcation when appropriate parameters are changed. When this occurs, the system is said to be excitable[3]. When a system is excitable, perturbations larger than the threshold (super-threshold perturbations) cause the trajectory to make a large phase space excursion, called an excitation cycle.

In contrast, excitation behaviour is absent during direct convergence to the linearly stable equilibrium following a sub-threshold disturbance. Here, the stable manifold of the newly developing saddle-node serves as the excitation threshold[3–5]. Still other contributions turn to stochasticity, examining how environmental noise, regime switching, or fear-mediated behavioral responses interact with spatial diffusion to govern extinction, persistence, and long-run statistical equilibria[6]. Predator-prey model with prey-taxis is discussed in detail by Fan et al.[7]. Four-species delayed predator-prey system is studied by Jia et al.[8]. Others incorporate behavioral mechanisms such as prey-taxis and hunting cooperation, showing how directed movement toward or away from the opposing species can itself become a source of pattern formation or, conversely, a stabilizing force[9]. Lam and Lee studied the asymptotic spreading dynamic of predator-prey populations in shifting environment[10]. Finally, a growing literature addresses non-equilibrium and moving-habitat scenarios, using tools such as the Hamilton–Jacobi approach to characterize invasion and spreading speeds as environmental conditions shift in space and time[11]. Reaction-diffusion stochastic predator-prey system with fear effect is studied in detail[12]. The behavioral mechanisms, prey-taxis and hunting cooperation is also presented by Tao and Wang[13]. Diffusion has long occupied a central place in the mathematical study of predator–prey interactions, ever since Turing's insight that differential dispersal rates between interacting species can destabilize an otherwise stable equilibrium and generate self-organized spatial structure. In the years since, this basic observation has grown into a rich and still-expanding research program, one that recent work continues to push in new directions. Some studies extend the classical reaction-diffusion framework to heterogeneous or anisotropic habitats, where directional or spatially varying dispersal reshapes persistence and coexis-

tence outcomes [14]. A parallel body of work folds in ecological realism through delay, feedback control, disease transmission, or multi-species architectures, broadening single-pair models into more elaborate community-level systems [15]. Taken together, these threads illustrate that diffusion is no longer treated merely as a background transport process in predator–prey theory, but as an active ingredient whose interplay with behaviour, heterogeneity, and randomness continues to generate genuinely new dynamical phenomena. Recent studies have further demonstrated that fear-induced group defense and cooperative hunting can substantially modify predator–prey dynamics, producing complex bifurcation behavior, seasonal responses, uncertainty-driven changes, and spatio-temporal patterns [16].

In this research, the authors reveal that, over time, prey can drive predator extinction, accelerating the trade-off between food acquisition and safety in predator–prey ecology [17]. The authors discuss a predator-prey system, particularly in the context of cooperative hunting by the predator and the fear observed in the prey population [18]. The impact of group defense on the predator-prey system is studied by Pal et al. [19]. Their findings reveal that the parameters associated with group defence and predator-induced fear play vital roles in the survival and extinction of populations. Kim et al. found that fear of predators is triggered by predator aggregation, which in turn elicits an anti-predator response in the prey [20]. The authors consider cooperative hunting in generalist predators and group defense in prey within a mathematical framework to discuss the enormous diversity the system could encompass [21]. Backfiring is the term used to describe what happens when one pulse is moving in one direction, and another splits off and moves in the opposite direction [22]. In this research, the authors reveal, via numerical simulations, the emergence of a range of spatio-temporal patterns. They also demonstrate the patterns transformation with changes in ecological and evolutionary factors [23].

Importantly, from an ecological point of view, the excitable nature of systems allows for prolonged coexistence in spatially explicit systems that would not otherwise be viable without these patterns. For instance, it can be used to gauge the likelihood of a biological invasion's success, which might have far-reaching consequences for ecosystems. Therefore, in-depth research into such models is necessary for a comprehensive understanding of many occurrences. The dynamics of a pure reaction-diffusion system in classical mechanics have been thoroughly investigated. If the matrix of diffusion coefficients is diagonal and all its diagonal elements are constants, then we have a classical pure reaction-diffusion system. In ecological terms, this indicates that the dispersal of any given species is determined only by its gradient. This is a crucial assumption in environmental settings, and relaxing it can drastically alter the results of time-series models. It was recently demonstrated that cross-diffusion in a Bonhoeffer-van der Pol model can result in isolated pulses or wave trains [24]. The phrase "wave train" refers to a series of such pulses, while the word "solitary pulse" refers to a single travelling pulse reflecting a homoclinic solution [24]. The inhomogeneity of diffusivities in a Gray-Scott model with varied diffusion coefficients can dampen self-replicating behavior [25]. Advection can also cause wave trains to form in a model with Dirichlet boundary conditions [26]. Due to geographical segregation, it was found that competing populations can coexist in ecological situations through movement responses to environmental gradients [27]. In a more recent study, the authors discussed that using taxis as a factor in a competitive system can also impact the success of an invasion. Prey taxis, in which predator movement depends on the prey density gradient, is a more typical example of an ecological rationale for the existence of a non-diagonal diffusion matrix [28]. A concise summary of the effects of pursuit-evasion dynamics on biological invasions [29]. Bate studied the effect of prey-taxis on the velocity of propagating waves [30]. The authors discussed pattern formation and/or predator-prey taxis, and stability and bifurcation were studied in these papers [31–33]. No research on whether such a circumstance occurs within a practical range of parameters in an ecological system has been included in the theoretical justification. In addition, unlike in conventional reaction-diffusion systems, the effects of non-diagonal diffusion coefficient matrices (cross-diffusion) in ecological systems have not been extensively studied. Most spatially explicit models (especially those based on partial differential equations) assume that prey and predators only move by diffusion. This means that predators and prey act arbitrarily, uninfluenced by outside factors. However, motion is rarely haphazard. Prey and predators are attracted to and repelled by a variety of environmental gradients, including those of chemical attractants and repellents (chemotaxis), oxygen concentra-

tion (aerotaxis), and prey density (prey-taxis). In their work modelling the foraging behaviour of Ladybugs, the authors developed the term ”prey-taxis”[34]. To model prey-taxis, researchers can take a “direct” or ”indirect” approach[35]. The term ”direct prey-taxis” refers to the incorporation of a flux in the predator dynamics that is dependent on gradients of prey density[34,36–39], while the term ”indirect prey-taxis” refers to the incorporation of a separate predator velocity equation where predators accelerate according to prey gradients. So, in direct prey-taxis, the predator’s speed is directly proportional to the gradients of available prey (similar to the formulation of other classical taxis models, such as chemotaxis). Still, in indirect prey-taxis, the predator speeds up to match the gradients in the availability of prey. It appears that these two approaches to modelling prey-taxis produce contradictory outcomes. The stabilizing impact of direct prey-taxis limits the spatiotemporal chaos and oscillations induced by intense prey-taxis[38]. However, this is only possible for moderate (and appealing) prey-taxis values when using indirect prey-taxis[40]. Some ‘inertia’ or delay may account for this distinction in indirect prey-taxis; once predators reach the peak of prey density, they stop accelerating but retain their velocity, allowing them to overshoot their target. While many studies have examined the role of prey-taxis in pest control[40], most have instead focused on pattern development[41]. The spatial and temporal variations of the predator’s velocity are discussed by the prey gradient[39]. The authors introduced prey-taxis into the Previte–Hoffman model and investigated steady-state bifurcation under no-flux boundary conditions. They analysed the stability of the positive equilibrium, the Hopf bifurcation, and the steady-state bifurcation. Using Crandall–Rabinowitz’s local bifurcation theory, they studied the existence and stability of nonconstant steady states resulting from the bifurcation[42]. The authors explored prey-taxis in an ecological model by investigating a predator-prey system[43]. They studied the local stability of the positive equilibrium and the conditions for steady-state bifurcation. Then, they investigated the existence and stability of the bifurcating solution near the threshold. Chen, Mengxin, and Ranchao Wu[44] made a valuable contribution to understanding how predator-taxis influence a predator–prey model with Michaelis–Menten-type nonlinear harvesting. They established the local and global existence, and the boundedness, of solutions to the system through theoretical analysis of quasilinear parabolic equations. Chen, M., and Srivastava, H.[45] were interested in a chemotaxis model with no-flux boundary conditions. The authors investigated the stability of the singular positive steady state, both as a parameter for Hopf bifurcation and for steady-state bifurcation, with respect to the chemotaxis coefficient. Then, using the Crandall-Rabinowitz local bifurcation theory, the existence and stability of the bifurcating solution from the steady-state bifurcation are investigated.

Novelty and Main Contributions

Although predator-prey models, reaction-diffusion equations, group-defence mechanisms, and numerical finite-difference methods have each been extensively investigated, relatively few studies integrate all these components into a single mathematical framework. The novelty of the present work lies not in introducing an entirely new ecological process, but in developing a comprehensive mathematical model that simultaneously incorporates environmental regulation of prey group defense, spatial diffusion, rigorous analytical investigation, and efficient numerical computation. The present study makes the following key contributions:

(1) An environmentally regulated logistic group-defense function is used to model adaptive prey defense under varying environmental conditions in a three-species predator-prey model.

(2) The model is developed to incorporate diffusion to study both temporal and spatial predator-prey dynamics in heterogeneous habitats.

(3) Theoretical analyses establish the positivity, boundedness, existence, and local and global stability of the proposed ecological model.

(4) A new explicit three-level finite difference scheme is developed to solve the nonlinear reaction-diffusion system with second-order temporal accuracy efficiently.

(5) The proposed numerical method is validated through Von Neumann stability analysis and tests of nonlinear convergence, positivity, and boundedness.

(6) Numerical simulations demonstrate the roles of environmental regulation and group defence in species coexistence, ecosystem stability, and biodiversity conservation.

The proposed framework unifies environmental reg-

ulation, diffusion, stability analysis, and efficient numerical approximation within a single predator-prey modelling framework. In **Table 1**, we present a comparison of the present work with representative studies in the literature.

Table 1. Comparison of the present work with representative studies in the literature.

Existing Literature	Representative References	Present Work
Predator-prey models with constant group-defense functions, where prey defense is assumed fixed or depends only on predator density.	Cosner et al. [46]; Li et al. [47]; Berezovskaya et al. [48]	Introduces an environmentally regulated group-defence mechanism via a logistic function, allowing defence intensity to vary continuously with environmental conditions.
Classical reaction-diffusion predator-prey models emphasizing diffusion-driven coexistence and spatial pattern formation without environmental regulation of defense.	Murray [49]; Cantrell and Cosner [50]; Okubo and Levin [51]	Develops a reaction-diffusion model in which environmental drivers directly regulate collective defense, thereby influencing both temporal and spatial population dynamics.
Traditional three-species ecological models involving two prey and one predator but neglecting environmentally dependent collective defense.	Freedman [52]; Hsu et al. [53]; Chattopadhyay and Arino [54]	Proposes a three-species ecological system integrating two prey populations, one predator, diffusion, and environmentally controlled group-defense mechanisms within a unified framework.
Stability analyses primarily focused on equilibrium existence or local stability using Jacobian eigenvalues.	Perko [55]; Hofbauer and Sigmund [56]	Provides a complete qualitative analysis, including positivity, boundedness, equilibrium existence, local stability via the Routh-Hurwitz criterion, and global stability using a Lyapunov function.
Numerical studies employing conventional finite difference or finite element methods with limited stability analysis.	Morton and Mayers [57]; LeVeque [58]; Smith [59]	Develops a new explicit three-level finite difference scheme, derives the unknown coefficients using Taylor series expansion, performs Von Neumann stability analysis, and verifies nonlinear convergence numerically through mesh-refinement studies.
Ecological models discussing diffusion or group defense separately.	Roy et al. [60]	Integrates environmental regulation, group defense, reaction-diffusion dynamics, analytical stability theory, and numerical computation within a single mathematical framework.

The present study focuses on the combined effects of environmental drivers, prey-group defence, and spatial diffusion in a three-species predator-prey system comprising two prey populations and one predator population. Unlike many existing studies that consider only homogeneous environments or single-prey interactions, the proposed model incorporates an environmentally regulated group-defence mechanism and random spatial movement via diffusion. The mathematical analysis establishes positivity, boundedness, the existence of an equilibrium, and both local and global stability conditions for the non-diffusive system. The reaction-diffusion extension is then investigated using Fourier analysis and the Routh-Hurwitz criterion. At the same time, a three-level finite difference scheme is developed and analysed using the Von Neumann stability analysis.

Although a large body of literature exists on predator-prey systems with group defence and reaction-diffusion dynamics, several important limitations remain. Many pre-existing models assume that prey protection is constant and ignore environmental influences on prey protection strategies. Moreover, a few studies have integrated, within a single modelling framework, the simultaneous inclusion of environmentally regulated group defence, multiple prey species, spatial dispersal, comprehensive stability analysis, and efficient numerical approximation. These restrictions motivate the present work. The main goal of this study is to develop and analyse a reaction-diffusion predator-prey model that incorporates group defence in the presence of the environment, identify the qualitative properties of the resulting system of equations, and construct an accurate three-level finite-difference scheme to study the spatiotemporal dynamics of the system. The suggested framework offers both mathematical and ecological perspectives on the role of environmental variability in predator-prey coexistence and ecosystem stability.

The study is organized as a series of sections. Section 2 presents a three-species ecological model, explains the model parameters, and demonstrates the influence of group defence on predation rates. In Section 3, the model is analysed, including positivity and boundedness, identification of equilibrium points, existence conditions for equilibrium points, local/global stability analysis based on the Routh-Hurwitz criterion, and a Volterra-type Lyapunov function. In Section 4, a diffusion system related to the model is introduced, and its stability is analysed. In Section 5, an explicit numerical scheme for the simulation and analysis

of the model/diffusion system is constructed, and the Von Neumann criterion is used to analyse it. The findings are thoroughly discussed in Section 6. Finally, in Section 7, a brief conclusion summarizes the key findings and indicates future research directions.

2. The Model

Ordinary differential equations are efficiently used to model predator-prey interaction. Several factors play a crucial role in determining the system's complexity. Here, we define a three-species predator-prey model that incorporates the impact of group defense. Group defense is a strategy that the prey use to reduce the risk of attack. Group defence by prey species is a captivating survival strategy observed in the animal kingdom, in which individuals collectively thwart their natural enemies' predatory advances. This astonishing phenomenon manifests as a coordinated effort among members of a prey species to reduce the overall risk of predation. These prey species find safety in numbers, often through synchronised behaviours such as flocking, schooling, or herding. Grouping makes it much harder for predators to take out a single prey item and provides a strong defence against potential predators. Predator limitation – predators are unable to attack more than one prey item at a time, and the confusion and complexity of prey groups provide protection not available to prey individuals in isolation. This approach increases the likelihood that individual prey survive and highlights how remarkable it is that animals can be so adaptable and social. We consider three species models in this study, comprising two prey species and a predator species. The model is described below

$$\begin{aligned}\frac{dP}{dt} &= r_1 P\left(1-\frac{P}{K_1}\right)\\ &-\alpha_1 PN\left(1-\frac{G_{max}}{1+e^{-K(D-D_0)}}\right),\ t>0\end{aligned} \tag{1}$$

$$\begin{aligned}\frac{dQ}{dt} &= r_2 Q\left(1-\frac{Q}{K_2}\right)\\ &-\alpha_2 QN\left(1-\frac{G_{max}}{1+e^{-K(D-D_0)}}\right),\ t>0\end{aligned} \tag{2}$$

$$\begin{aligned}\frac{dN}{dt} &= N\left(\beta_1 P+\beta_2 Q\right)\left(1-\frac{G_{max}}{1+e^{-K(D-D_0)}}\right)\\ &-\delta N,\ t>0\end{aligned} \tag{3}$$

with the following initial conditions

$$P(0)\geq 0, Q(0)\geq 0, N(0)\geq 0. \tag{4}$$

The parameters are considered non-negative, and their physical meanings and notations are presented in **Table 2**.

Table 2. Parameters and their physical meanings.

Parameters	Physical Meanings
P	Population density of prey-1
Q	Population density of prey-2
N	Predator's population density
r_1	Intrinsic growth rate for P
r_2	Intrinsic growth rate for Q
K_1	Carrying capacity for P
K_2	Carrying capacity for Q
G_{max}	Maximum level of group defense
α_1	Attack rate of the predator on prey species P
α_2	Attack rate of the predator on prey species Q
D_0	Threshold value of the environmental driving factor at which group defense increases significantly
D	Normalized environmental suitability or driving factor representing resource availability, habitat quality, temperature suitability, vegetation cover, and predation pressure.
K	Steepness parameter controlling the sensitivity of group defense to changes in D
δ	Death rate for predator
β_1	Conversion rate of P to N
β_2	Conversion rate of Q to

To account for environmentally regulated collective behaviour, the predator-prey interactions are modified by the group-defence function G, which adjusts the effective predation intensity based on habitat quality and environmental conditions.

For the sake of simplicity, we rewrite the above system

(1)–(3) as

$$\frac{dP}{dt} = r_1 P\left(1 - \frac{P}{K_1}\right) - \alpha_1 PN(1-G), t > 0 \quad (5)$$

$$\frac{dQ}{dt} = r_2 Q\left(1 - \frac{Q}{K_2}\right) - \alpha_2 QN(1-G), t > 0 \quad (6)$$

$$\frac{dN}{dt} = N\left(\beta_1 P + \beta_2 Q\right)(1-G) - \delta N, t > 0 \quad (7)$$

where $G = \frac{G_{max}}{1+e^{-K(D-D_0)}}$.

Here G depends on several factors like $G_{max},\ D,\ D_0$ and K. The factor G_{max} represents the maximum level of group defense that can be achieved. This factor sets the upper limit on how effectively the prey can defend themselves, given the increased driving factor. D_0 determines the value of D at which group defense starts to increase significantly. It represents a threshold point in the group defense response to changes in the driving factor. Identifying this threshold can help understand when and how prey exhibit group defense behaviour. The next factor K is taken to control the steepness of the logistic curve. It determines how rapidly group defense changes in response to changes in the driving factor. A higher value of K makes the transition from low to high group defense steeper, while a lower value makes it more gradual. The choice of K influences the sensitivity of group defense to changes in the driving factor. The driving factor D represents the external variable that influences group defense.

The equation $\frac{G_{max}}{1+e^{-K(D-D_0)}}$ within the model, the dynamics of prey group defense in response to environmental stimuli are captured. Here, G_{max} signifies the maximum achievable defense level, while D_0 marks the point at which defense mechanisms considerably intensify. The parameter K controls the steepness of the curve, determining how promptly defense levels react to changes in the environmental factor D. Essentially, D embodies the external influence shaping the vigour of group defense, whether it be resource abundance, habitat conditions, or predator presence. This model formulation provides a valuable understanding of how environmental variations affect the interplay between prey and predators, revealing the complexity of collective defense strategies and their vulnerability to environmental fluctuations.

2.1. Biological Interpretation of the Group-Defense Function

The logistic group defense function is used because it resembles one of the most noted behavioural responses in ecological systems: an increase in group defense with a threshold. Prey do not quickly acquire high defense levels in natural populations as conditions improve. In general, collective defense takes three steps.

When environmental conditions are poor (poor food supply, degraded habitats, physiological stress, etc.), prey generally do not aggregate into large, cohesive schools of fish. Therefore, the level of collective defense is low. When environmental conditions improve and exceed a critical threshold, prey can more effectively form cohesive groups through herding, schooling, flocking, or coordinated vigilance. This shift may be fast, as larger and healthier populations can invest more in anti-predator strategies. Finally, as environmental conditions become very favourable, the effectiveness of collective defense approaches an upper bound, as behavioural coordination, communication, and group organisation cannot grow beyond a certain point. The logistic function has a lower plateau representing these three ecological phases, a transition region, and an upper plateau representing saturation.

The environmental driving factor D is therefore interpreted as a normalized environmental suitability index rather than a single measurable variable. In practice, D may be estimated from one or more ecological indicators, including vegetation biomass, prey density, food availability, habitat quality, climatic suitability, water availability, or predator pressure. Depending on the ecosystem under consideration, these variables may be combined into a dimensionless environmental index ranging from unfavourable to highly favourable conditions. The threshold parameter D_0 represents the environmental condition at which collective defense begins to increase rapidly, while the parameter K determines how sensitive prey behaviour is to environmental change.

In addition, many empirical observations across a wide range of ecological systems support the proposed functional response. Fish schools are more cohesive under better environmental conditions and higher predator risk. Likewise, many bird species tend to aggregate more when food is abundant, and ungulates like wildebeest, zebra, muskox and

caribou do the same when habitat conditions allow sufficient aggregation to provide them with adequate protection. Collective defense builds up quickly after favourable environmental conditions are reached and ultimately reaches a biological maximum, although the exact behavioural mechanisms vary from species to species. The logistic function is therefore biologically realistic and mathematically flexible, as it represents group defense in various ecological systems in a manner regulated by environmental factors.

The present model is therefore intended to represent this general ecological principle rather than the behaviour of a single species. The logistic formulation provides a continuous and bounded description of collective defense that is consistent with observed threshold responses in many social prey populations while remaining sufficiently general to accommodate different ecosystems through appropriate parameter selection.

In the present model, the driving factor D is biologically interpreted as a normalized environmental suitability index. It represents the combined influence of resource availability, habitat quality, temperature suitability, vegetation cover, and predation pressure on prey populations' ability to organise collective defense. Thus, D is not a single physical quantity, but a composite ecological indicator. Low values of D correspond to unfavourable environmental conditions, such as limited food supply, poor habitat structure, extreme temperatures, or high environmental stress, in which prey individuals are less able to form effective defensive groups. Moderate values of D represent intermediate ecological conditions, while high values of D describe favourable habitats where prey can aggregate, coordinate movement, and exhibit stronger collective defense. Accordingly, the group-defense function is written as: $\frac{G_{max}}{1+e^{-K(D-D_0)}}$. Here, G_{max} denotes the maximum attainable level of group defence, D_0 is the environmental threshold at which group defense begins to increase significantly, and K controls the steepness or sensitivity of the defensive response to changes in D.

In the numerical simulations, the values $G = 0.1$, $G = 0.4$, and $G = 0.7$ are interpreted as weak, moderate, and strong group-defense levels, respectively. These values correspond to poor, intermediate, and favourable environmental conditions. For biological feasibility, we assume: $0 \leq G < G_{max} \leq 1$. This assumption ensures that the effective predation term, written as $(1 - G)$, remains non-negative.

Here are examples showing the influence of key parameters on the level of group defense G in the model:

1. High G_{max}, $D > D_0$, High K:
   Illustration: In scenarios where the maximum defense capacity G_{max} is set to 1.0, and the environmental variable D significantly exceeds the threshold point D_0 by a factor of 2, with a steep sensitivity parameter K at 2.0, the resulting level of group defense G approximates 0.92. This demonstrates the robust defense response of prey populations to favourable environmental conditions, in which high resource availability leads to the development of heightened defense mechanisms.
2. Moderate G_{max}, $D \approx D_0$, Moderate K:
   Illustration: Consider a scenario with a moderately high maximum defense capacity G_{max} set to 0.8, where the environmental variable D closely approximates the threshold point D_0 at 5.0, alongside a moderate sensitivity parameter K of 1.5. Under these conditions, the resulting level of group defense G is approximately 0.67. This indicates a balanced response of prey populations to environmental cues, where defence mechanisms are activated in proportion to resource availability without reaching their maximal capacity.
3. Low G_{max}, $D < D_0$, Low K:
   Illustration: In scenarios characterized by low maximum defense capacity G_{max} at 0.5, where the environmental variable D falls below the threshold point D_0 by a factor of 2, coupled with a low sensitivity parameter K of 0.8, the resulting level of group defense G is approximately 0.12. This exemplifies a subdued defense response of prey populations to unfavourable environmental conditions, where limited resources prevent the activation of robust defense mechanisms.

In **Figure 1**, the environmental driving factor is shown to affect the prey group-defense function, as illustrated in this figure. The logistic response demonstrates the effect of improving environmental conditions on collective defensive behaviour. As the driving factor increases, group defense increases, decreasing prey vulnerability to predation and improving conditions for long-term species survival.

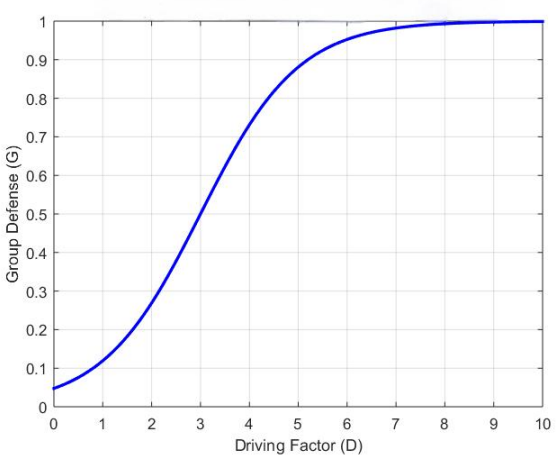

Figure 1. Impact of driving factor on group defense.

Figure 2 shows that environmental driving factor affects the results with varying threshold values for D. The simulations represent that changes in environmental sensitivity change the timing and intensity of collective defense. A higher threshold leads to a later onset of effective defense mechanisms, so that prey are exposed to predators when the environment is more unfavourable.

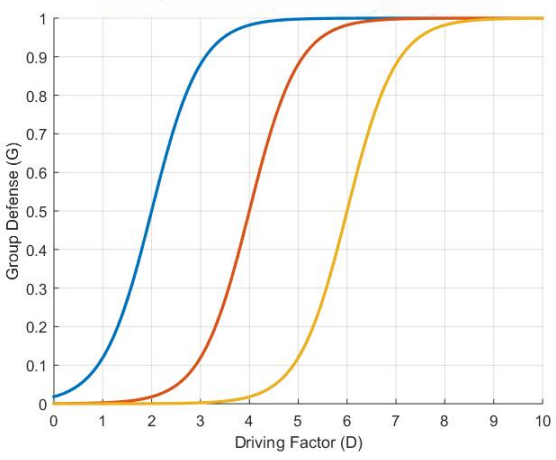

Figure 2. Impact of varying driving factors on group defense.

2.2. Model Assumptions and Limitations

Several simplifying assumptions are made in the development of the proposed predator-prey model that allow for its mathematical analysis while still retaining the important ecological mechanisms of interest. These assumptions are common in ecological modelling but can always affect the interpretation and applicability of the results.

First, the prey population is assumed to grow logistically, as is the predator population. This assumption is based on the concept of density-dependent population regulation driven by limited resources, habitat availability, and intraspecific competition. Logistic growth is one of the most widely used population growth models because it is realistic and exhibits population saturation in an environment with finite carrying capacity. However, the growth patterns for natural populations can be more complicated: Allee effects, age structure, delayed density dependence, and resource-dependent carrying capacities are not included in the present study.

Second, predator mortality is modelled as a constant per capita mortality rate. This assumption greatly simplifies predator dynamics and is applicable when the natural death rate is the dominant cause of predator deaths, and changes in predator numbers are slow compared to those in prey numbers. The environment, disease, food availability, or population density may also influence predator mortality. The introduction of density-dependent or environmentally dependent mortality (population-level) could lead to further ecological behaviours and is a promising path to explore in future research.

Third, the prey-to-predator conversion efficiencies are assumed to remain constant throughout the simulation. This implies that predators convert consumed prey into reproductive success with fixed efficiency. Conversion efficiency may vary with prey quality, predator age, nutritional status, seasonal conditions, or environmental stress. Allowing variable conversion efficiencies would increase biological realism but would also introduce additional parameters and analytical complexity.

Fourth, spatial movement is represented by homogeneous diffusion with constant diffusion coefficients. This assumption models random movement in a spatially uniform environment and provides a standard description of dispersal in reaction-diffusion systems. In heterogeneous landscapes, however, movement rates often depend on habitat quality, environmental gradients, resource availability, or behavioural responses. Future studies could represent such processes using heterogeneous, density-dependent, or anisotropic diffusion coefficients.

Fifth, the current model is deterministic and does not explicitly account for environmental stochasticity. Environmental fluctuations arising from climate variability, drought, disease outbreaks, or extreme weather events may substan-

tially affect predator-prey interactions, particularly in small populations. Although deterministic models provide important baseline insights into ecological dynamics, stochastic formulations may offer a more realistic description of uncertain environmental conditions and deserve further investigation.

Last, the current formulation does not include seasonal forcing. Therefore, the growth rates, predation rates, and environmental conditions are assumed to remain constant throughout the simulation. Seasonal changes in temperature, precipitation, food availability and breeding activity for many natural systems can affect predator-prey relationships. Periodic environmental forcing may reveal other behaviours, such as oscillations, resonance, and periodic coexistence.

Finally, the two prey populations interact only indirectly through their common predator, and direct competition for shared resources is neglected. This assumption allows the present study to isolate the effects of environmentally regulated group defense and spatial diffusion without introducing additional interaction mechanisms. In ecosystems where prey species compete strongly for food, shelter, or breeding sites, direct interspecific competition could alter coexistence conditions and should be incorporated in future extensions of the model.

Despite these simplifying assumptions, the proposed model captures the principal ecological processes motivating this study: environmental regulation of collective defense, predator-prey interactions, and spatial dispersal. The analytical and numerical results therefore provide a useful baseline for understanding environmentally driven predator-prey dynamics, while also establishing a mathematical framework that can be extended to include stochasticity, heterogeneous environments, seasonal forcing, interspecific competition, and adaptive behavioural responses in future research.

3. Analysis of the Model

In this section, we present the positivity and boundedness of the solution to the system (1)–(3). Equilibrium points, along with the stability of the coexistence point, are discussed in the same section.

Theorem 1. *For any initial condition* $P(0) \geq 0,\ Q(0) \geq 0,$ and $N(0) \geq 0$*, the system admits a unique non-negative solution.*

Proof. The right-hand sides of the model are continuously differentiable functions of $P,\ Q$, and N in the non-negative region R^3_+. Therefore, by the standard existence and uniqueness theorem for ordinary differential equations, there exists a unique local solution corresponding to each non-negative initial condition.

To prove positivity, the first equation of system (5)–(7) gives the following result:

$$\frac{dP}{dt} = r_1 P\left(1 - \frac{P}{K_1}\right) - \alpha_1 PN(1-G).$$

Hence, we have

$$P(t) = P(0)exp\left[\int_0^t \left(r_1\left(1 - \frac{P(\theta)}{K_1}\right) - \alpha_1 N(\theta)(1-G)\right)d\theta\right],$$

Since $P(0) \geq 0$, it follows that $P(t) \geq 0$ for all $t \geq 0$

$$\Rightarrow\ P(t) \geq 0. \tag{8}$$

Similarly, Equation (2) results in the following.

$$\frac{dQ}{dt} = r_2 Q\left(1 - \frac{Q}{K_2}\right) - \alpha_2 QN(1-G),$$

$$Q(t) = Q(0)exp\left[\int_0^t \left(r_2\left(1 - \frac{Q(\theta)}{K_2}\right) - \alpha_2 N(\theta)(1-G)\right)d\theta\right],$$

which gives $Q(t) \geq 0$ for all $t \geq 0$.

$$\Rightarrow\ Q(t) \geq 0. \tag{9}$$

Now, Equation (3) gives us.

$$\frac{dN}{dt} = N\left(\beta_1 P + \beta_2 Q\right)(1-G) - \delta N,$$

$$N(t) = N(0)exp\left[\int_0^t \left(\left(\beta_1 P(\theta) + \beta_2 Q(\theta)\right)(1-G) - \delta\right)d\theta\right],$$

Thus, $N(t) \geq 0$ for all $t \geq 0$.

$$\Rightarrow\ N(t) \geq 0 \tag{10}$$

Therefore, every solution starting in R^3_+ remains in R^3_+. □

Theorem 2. *All non-negative solutions of the system are bounded.*

Proof. Since $0 \leq G < 1$, the prey equations satisfy

$$\frac{dP}{dt} \leq r_1 P(1 - \frac{P}{K_1}),$$

and

$$\frac{dQ}{dt} \leq r_2 Q\left(1 - \frac{Q}{K_2}\right).$$

By the comparison theorem, $P(t) \leq max\left\{P(0),\ K_1\right\}$, and $Q(t) \leq max\{Q(0),\ K_2\}$.

Thus, both prey populations are bounded.

To prove boundedness of the predator population, define the weighted total population function: $W(t) = P(t) + Q(t) + \eta N(t)$, where $\eta > 0$ is chosen such that: $\eta\beta_1 \leq \alpha_1$, and $\eta\beta_2 \leq \alpha_2$. Differentiating $W(t)$, we obtain:

$$\frac{dW}{dt} = \frac{dP}{dt} + \frac{dQ}{dt} + \eta\frac{dN}{dt}. \tag{11}$$

Using the model equations, this gives:

$$\begin{gathered}\frac{dW}{dt} = r_1 P(1 - \frac{P}{K_1}) + r_2 Q(1 - \frac{Q}{K_2}) \\ -(\alpha_1 - \eta\beta_1)PN(1 - G) \\ -(\alpha_2 - \eta\beta_2)QN(1 - G) - \eta\delta N.\end{gathered}$$

Since $\eta\beta_1 \leq \alpha_1$ and $\eta\beta_2 \leq \alpha_2$, the interaction terms are non-positive. Therefore,

$$\frac{dW}{dt} \leq r_1 P(1 - \frac{P}{K_1}) + r_2 Q(1 - \frac{Q}{K_2}) - \eta\delta N. \tag{12}$$

For some positive constants μ and C, this implies

$$\frac{dW}{dt} + \mu W \leq C.$$

Hence, by Gronwall's inequality,

$$W(t) \leq W(0)e^{-\mu t} + \frac{C}{\mu}[1 - e^{-\mu t}]. \tag{13}$$

Therefore, $W(t) \leq max\{W(0), \frac{C}{\mu}\}$.

Since P, Q, and N are non-negative, this proves that all populations are bounded. Equations (11)–(13) provide the result. □

3.1. Stability Analysis of the Model

This section deals with the analysis of the model (5)–(7). We solve the following system of equations to find the equilibrium points

$$0 = r_1 P\left(1 - \frac{P}{K_1}\right) - \alpha_1 PN(1 - G), \tag{14}$$

$$0 = r_2 Q\left(1 - \frac{Q}{K_2}\right) - \alpha_2 QN(1 - G), \tag{15}$$

$$0 = N\left(\beta_1 P + \beta_2 Q\right)(1 - G) - \delta N. \tag{16}$$

We get the following fixed points to solve the above system (14)–(16).

i. Prey-1, predator-free equilibrium point:

$$E_1 = (0, K_2, 0)$$

This equilibrium point exists under no additional condition as $K_2 > 0$.

ii. Predator-free equilibrium point:

$$E_2 = (K_1, K_2, 0)$$

The predator-free equilibrium point always exists as K_1 , $K_2 > 0$.

iii. Prey-2, predator-free equilibrium point:

$$E_3 = (K_1, 0, 0)$$

The equilibrium point E_3 also exists as long as the carrying capacity is positive.

iv. Prey-1 free equilibrium point:

$$E_4 = \left(0, -\frac{\delta}{(-1+G)\beta_2}, -\frac{r_2(\delta - k_2\beta_2 + Gk_2\beta_2)}{(-1+G)^2 k_2\alpha_2\beta_2}\right)$$

This equilibrium point gives the extinction of prey-1. It exists if $G < 1$ and $k_2\beta_2 > \delta + Gk_2\beta_2$.

v. Coexistence equilibrium point:

$$E_5 = \left(\begin{array}{c} \frac{k_1(-\delta r_2\alpha_1 + (-1+G)k_2(-r_2\alpha_1 + r_1\alpha_2)\beta_2)}{(-1+G)(k_1 r_2\alpha_1\beta_1 + k_2 r_1\alpha_2\beta_2)}, \frac{k_2(-\delta r_1\alpha_2 + (-1+G)k_1(r_2\alpha_1 - r_1\alpha_2)\beta_1)}{(-1+G)(k_1 r_2\alpha_1\beta_1 + k_2 r_1\alpha_2\beta_2)}, \\ -\frac{r_1 r_2(\delta + (-1+G)k_1\beta_1 + (-1+G)k_2\beta_2)}{(-1+G)^2(k_1 r_2\alpha_1\beta_1 + k_2 r_1\alpha_2\beta_2)} \end{array} \right)$$

- This equilibrium point is the most important and requires some exciting conditions. The conditions are given under

$$\begin{cases} G < 1 \\ k_2 r_2 \alpha_1 \beta_2 < \delta r_2 \alpha_1 + k_2 r_1 \alpha_2 \beta_2 \\ k_1 r_1 \alpha_2 \beta_1 < \delta r_1 \alpha_2 + k_1 r_2 \alpha_1 \beta_1 \\ k_1 \beta_1 + k_2 \beta_2 > \delta \end{cases} \tag{17}$$

vi. Population-free equilibrium point:

$$E_6 = (0,\ 0,\ 0)$$

This equilibrium point suggests the destruction of the ecosystem, which is not biologically meaningful.

vii. Prey-2 free equilibrium point:

$$E_7 = \left(-\frac{\delta}{(-1+G)\beta_1},\ 0,\ -\frac{r_1(\delta - k_1\beta_1 + Gk_1\beta_1)}{(-1+G)^2 k_1 \alpha_1 \beta_1} \right)$$

The equilibrium point exists if $G < 1$ and $k_1\beta_1 > Gk_1\beta_1 + \delta$.

Theorem 3. *The coexistence equilibrium point is locally stable under the following conditions*

$$a_{22}a_{23}a_{32} > a_{11}\left(a_{22}\left(a_{11}+a_{22}\right) - a_{13}a_{31}\right),$$

$$a_{11} + a_{22} < 0,$$

$$a_{13}a_{22}a_{31} + a_{11}a_{23}a_{32} > 0,$$

$$a_{11}a_{22} > a_{13}a_{31} + a_{23}a_{32}.$$

Where,

$$a_{11} = \frac{r_1\left(\delta r_2\alpha_1 + (-1+G)k_2\left(r_2\alpha_1 - r_1\alpha_2\right)\beta_2\right)}{(-1+G)(k_1 r_2 \alpha_1 \beta_1 + k_2 r_1 \alpha_2 \beta_2)},$$

$$a_{13} = \frac{k_1\alpha_1(-\delta r_2\alpha_1 + (-1+G)k_2(-r_2\alpha_1 + r_1\alpha_2)\beta_2)}{k_1 r_2 \alpha_1 \beta_1 + k_2 r_1 \alpha_2 \beta_2},$$

$$a_{22} = \frac{r_2(\delta r_1\alpha_2 + (-1+G)k_1(-r_2\alpha_1 + r_1\alpha_2)\beta_1)}{(-1+G)(k_1 r_2 \alpha_1 \beta_1 + k_2 r_1 \alpha_2 \beta_2)},$$

$$a_{23} = \frac{k_2\alpha_2(-\delta r_1\alpha_2 + (-1+G)k_1(r_2\alpha_1 - r_1\alpha_2)\beta_1)}{k_1 r_2 \alpha_1 \beta_1 + k_2 r_1 \alpha_2 \beta_2},$$

$$a_{31} = \frac{r_1 r_2 \beta_1(\delta + (-1+G)k_1\beta_1 + (-1+G)k_2\beta_2)}{(-1+G)(k_1 r_2 \alpha_1 \beta_1 + k_2 r_1 \alpha_2 \beta_2)},$$

$$a_{32} = \frac{r_1 r_2 \beta_2(\delta + (-1+G)k_1\beta_1 + (-1+G)k_2\beta_2)}{(-1+G)(k_1 r_2 \alpha_1 \beta_1 + k_2 r_1 \alpha_2 \beta_2)}$$

Proof. First, we find the Jacobian for the system (1)–(3)

$$J = \begin{pmatrix} (1-\frac{P}{k_1})r_1 - \frac{Pr_1}{k_1} - (1-G)N\alpha_1 & 0 & (-1+G)P\alpha_1 \\ 0 & (1-\frac{Q}{k_2})r_2 - \frac{Qr_2}{k_2} - (1-G)N\alpha_2 & (-1+G)Q\alpha_2 \\ (1-G)N\beta_1 & (1-G)N\beta_2 & -\delta + (1-G)P\beta_1 + (1-G)Q\beta_2 \end{pmatrix}.$$

Computing the Jacobian at the coexistence equilibrium point, we obtain

$$J\left(E_5\right) = \begin{pmatrix} a_{11} & 0 & a_{13} \\ 0 & a_{22} & a_{23} \\ a_{31} & a_{32} & 0 \end{pmatrix}.$$

Here,

$$a_{11} = \frac{r_1(\delta r_2\alpha_1 + (-1+G)k_2(r_2\alpha_1 - r_1\alpha_2)\beta_2)}{(-1+G)(k_1 r_2 \alpha_1 \beta_1 + k_2 r_1 \alpha_2 \beta_2)},$$

$$a_{13} = \frac{k_1\alpha_1(-\delta r_2\alpha_1 + (-1+G)k_2(-r_2\alpha_1 + r_1\alpha_2)\beta_2)}{k_1 r_2 \alpha_1 \beta_1 + k_2 r_1 \alpha_2 \beta_2},$$

$$a_{22} = \frac{r_2(\delta r_1\alpha_2 + (-1+G)k_1(-r_2\alpha_1 + r_1\alpha_2)\beta_1)}{(-1+G)(k_1 r_2 \alpha_1 \beta_1 + k_2 r_1 \alpha_2 \beta_2)},$$

$$a_{23} = \frac{k_2\alpha_2(-\delta r_1\alpha_2 + (-1+G)k_1(r_2\alpha_1 - r_1\alpha_2)\beta_1)}{k_1 r_2 \alpha_1 \beta_1 + k_2 r_1 \alpha_2 \beta_2},$$

$$a_{31} = \frac{r_1 r_2 \beta_1(\delta + (-1+G)k_1\beta_1 + (-1+G)k_2\beta_2)}{(-1+G)(k_1 r_2 \alpha_1 \beta_1 + k_2 r_1 \alpha_2 \beta_2)},$$

$$a_{32} = \frac{r_1 r_2 \beta_2(\delta + (-1+G)k_1\beta_1 + (-1+G)k_2\beta_2)}{(-1+G)(k_1 r_2 \alpha_1 \beta_1 + k_2 r_1 \alpha_2 \beta_2)}.$$

Now, characteristic polynomials can be written as

$$\begin{gathered} \lambda^3 + \lambda^2\left(-a_{11} - a_{22}\right) + a_{13}a_{22}a_{31} + a_{11}a_{23}a_{32} \\ +\lambda\left(a_{11}a_{22} - a_{13}a_{31} - a_{23}a_{32}\right) = 0. \end{gathered} \tag{18}$$

The equilibrium point is stable according to the Routh Criterion if

$$a_{22}a_{23}a_{32} > a_{11}\left(a_{22}\left(a_{11}+a_{22}\right) - a_{13}a_{31}\right), \tag{19}$$

$$a_{11} + a_{22} < 0, \tag{20}$$

$$a_{13}a_{22}a_{31} + a_{11}a_{23}a_{32} > 0, \tag{21}$$

$$a_{11}a_{22} > a_{13}a_{31} + a_{23}a_{32}. \tag{22}$$

Hence, the theorem is proved. □

Theorem 4. *The Equations (1)–(3) are globally asymptotically stable for the coexistence equilibrium point* E_4 if $\alpha_i > \beta_i,\ i = 1, 2.$

Proof. Consider the following Lyapunov function for the coexistence equilibrium point

$$V(P,\,Q,\,N) = l_1\left(P - P^* - P^*\log\frac{P}{P^*}\right) + l_2\left(Q - Q^* - Q^*\log\frac{Q}{Q^*}\right) + l_3\left(N - N^* - N^*\log\frac{N}{N^*}\right) \tag{23}$$

Where l_1, l_2 and l_3 are positive constants whose value is to be determined. The derivative of the above equation leads to the following

$$\frac{dV}{dt} = l_1\left(1 - \frac{P^*}{P}\right)\frac{dP}{dt} + l_2\left(1 - \frac{Q^*}{Q}\right)\frac{dQ}{dt} + l_3\left(1 - \frac{N^*}{N}\right)\frac{dN}{dt}.$$

Some simplification of the above leads to

$$\frac{dV}{dt} = l_1\left(\frac{P-P^*}{P}\right)\frac{dP}{dt} + l_2\left(\frac{Q-Q^*}{Q}\right)\frac{dQ}{dt} + l_3\left(\frac{N-N^*}{N}\right)\frac{dN}{dt}.$$

$$\begin{aligned}\frac{dV}{dt} &= l_1\left(P-P^*\right)\left[r_1P\left(1-\frac{P}{K_1}\right) - \alpha_1PN(1-G)\right] \\ &+ l_2\left(Q-Q^*\right)\left[r_2Q\left(1-\frac{Q}{K_2}\right) - \alpha_2QN(1-G)\right] \\ &+ l_3\left(N-N^*\right)\left[N\left(\beta_1P+\beta_2Q\right)(1-G) - \delta N\right].\end{aligned} \tag{24}$$

$$\begin{aligned}&\text{As } r_1\left(1-\frac{P^*}{K_1}\right) - \alpha_1N^*(1-G) = 0 \\ &\Rightarrow r_1 = \frac{r_1P^*}{k_1} + \alpha_1N^*(1-G),\end{aligned} \tag{25}$$

$$\begin{aligned}&\text{also, } r_2\left(1-\frac{Q^*}{K_1}\right) - \alpha_2N^*(1-G) = 0 \\ &\Rightarrow r_2 = \frac{r_2Q^*}{K_2} + \alpha_2N^*(1-G),\end{aligned} \tag{26}$$

and

$$\begin{aligned}&\left(\beta_1P+\beta_2Q\right)(1-G) - \delta = 0 \\ &\Rightarrow \delta = \left(\beta_1P^*+\beta_2Q^*\right)(1-G).\end{aligned} \tag{27}$$

Using Equations (25)–(27) in Equation (24), we have

$$\begin{aligned}\frac{dV}{dt} &= l_1\left(P-P^*\right)\left[\frac{r_1p^*}{k_1} + \alpha_1N^*(1-G) - \frac{r_1P}{k_1} - \alpha_1N(1-G)\right] \\ &+ l_2\left(Q-Q^*\right]\left[\frac{r_2Q^*}{K_2} + \alpha_2N^*(1-G) - \frac{r_2Q}{K_2} - \alpha_2N(1-G)\right] \\ &+ l_3\left(N-N^*\right)\left[\left(\beta_1P+\beta_2Q\right)(1-G) - \left(\beta_1P^*+\beta_2Q^*\right)(1-G)\right],\end{aligned} \tag{28}$$

$$\begin{aligned}\frac{dV}{dt} &= l_1\left(P-P^*\right)\left[-\frac{r_1}{k_1}\left(P-P^*\right) - \alpha_1(1-G)\left(N-N^*\right)\right] + \\ &l_2\left(Q-Q^*\right)\left[\frac{-r_2}{k_2}(Q-Q^*) - \alpha_2(1-G)\left(N-N^*\right)\right] \\ &+ l_3\left(N-N^*\right)\left[\beta_1\left(P-P^*\right)(1-G) + \beta_2\left(Q-Q^*\right)(1-G)\right].\end{aligned} \tag{29}$$

For simplicity, we assume that

$$l_1 = l_2 = l_3 = 1.$$

Using these values, Equation (24) leads to the following

$$\begin{aligned}\frac{dV}{dt} &= -\frac{r_1}{k_1}\left(P-P^*\right)^2 - \alpha_1\left(P-P^*\right)\left(N-N^*\right)(1-G) \\ &- \frac{r_2}{K_2}\left(Q-Q^*\right)^2 - \alpha_2\left(Q-Q^*\right)\left(N-N^*\right)(1-G) \\ &+ \beta_1\left(P-P^*\right)\left(N-N^*\right)(1-G) \\ &+ \beta_2\left(Q-\dot{Q}^*\right)\left(N-N^*\right)(1-G).\end{aligned} \tag{30}$$

Some simplification leads to

$$\begin{aligned}\frac{dV}{dt} &= -\frac{r_1}{k_1}\left(P-P^*\right)^2 - \frac{r_2}{k_2}\left(Q-Q^*\right)^2 \\ &- \left(\alpha_1-\beta_1\right)(1-G)\left(P-P^*\right)\left(N-N^*\right) \\ &- \left(\alpha_2-\beta_2\right)(1-G)\left(P-P^*\right)\left(N-N^*\right).\end{aligned}$$

$$\begin{aligned}&\Rightarrow \frac{dV}{dt} < 0 \text{ when } \alpha_1-\beta_1 > 0 \\ &\Rightarrow \alpha_1 > \beta_1 \;\&\; \\ &\alpha_2-\beta_2 > 0 \Rightarrow \alpha_2 > \beta_2\end{aligned} \tag{31}$$

Hence, the theorem is proved. □

3.2. Remark on the condition α_i and β_i

The condition $\alpha_1 > \beta_1$ and $\alpha_2 > \beta_2$ was imposed to make the Lyapunov derivative negative. Ecologically, this condition means that the predator's pressure on each prey population exceeds the conversion efficiency of consumed prey into predator biomass. In other words, predation removes prey more strongly than it contributes to predator growth. However, this condition can be restrictive because α_i and β_i may have different ecological scales. Therefore, we use suitable Lyapunov weights to avoid this unnecessary restriction. For the coexistence equilibrium $E^* = (P^*,\,Q^*,\,N^*)$, consider the Lyapunov function:

$$\begin{aligned}V(P,Q,N) &= l_1[P - P^* - P^*\ln(\tfrac{P}{P^*})] \\ &+ l_2[Q - Q^* - Q^*\ln(\tfrac{Q}{Q^*})] \\ &+ l_3[N - N^* - N^*\ln(\tfrac{N}{N^*})],\end{aligned}$$

where $l_1,\ l_2$, and l_3 are positive constants. Choose: $l_1 = \frac{\beta_1}{\alpha_1},\ l_2 = \frac{\beta_2}{\alpha_2},\ l_3 = 1$.

Then the mixed terms in the derivative cancel, and we obtain: $\frac{\beta_1 r_1}{\alpha_1 K_1}$

$$\frac{dV}{dt} = -\frac{\beta_1 r_1}{\alpha_1 K_1}(P-P^*)^2 - \frac{\beta_2 r_2}{\alpha_2 K_2}(Q-Q^*)^2 \le 0.$$

Thus, V is non-increasing. Moreover, $\frac{dV}{dt} = 0$ only when $P = P^*$ and $Q = Q^*$. Substituting $P = P^*$ and $Q = Q^*$ into the model equations gives $N = N^*$. Hence, by LaSalle's invariance principle, the coexistence equilibrium E^* is globally asymptotically stable in the positive region, provided that E^* exists and $0 \le G < 1$.

Figure 3 shows that weak group defense provides limited protection against predation, resulting in pronounced predator-prey oscillations before the populations converge to coexistence.

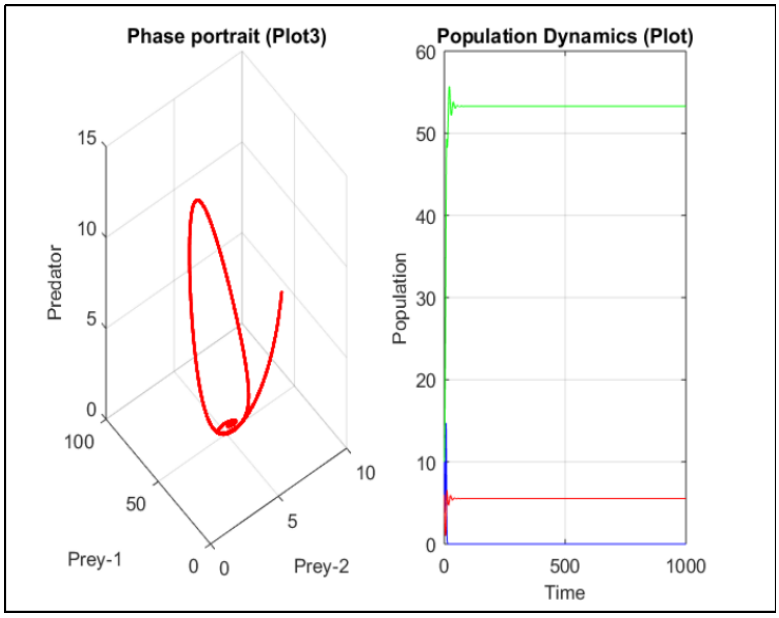

Figure 3. Phase portrait and time-series solution depicting the coexistence equilibrium for $G = 0.10$.

Figure 4 shows the coexistence equilibrium for $G = 0.30$, with its associated time-series solution, for the case where the solution is no longer unique. The larger the group of defenses, the less efficient predation becomes, resulting in smaller fluctuations in predator and prey populations and greater stability of the predator-prey relationship. The results show that moderate collective defense leads to an increase in ecosystem stability.

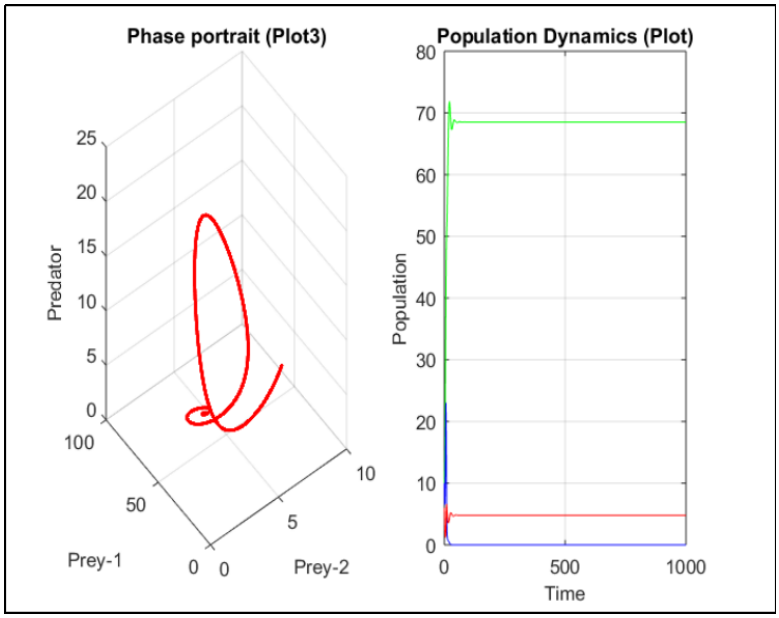

Figure 4. Phase portrait and time-series solution depicting the coexistence equilibrium for $G = 0.30$.

For $G = 0.50$, the coexistence equilibrium occurs on the phase portrait and is also captured in a time-series solution displayed in **Figure 5**. Collective defense significantly reduces predator success, while increasing prey counter-hunt success, enabling prey populations to recover and predator populations to persist. The system reaches a more stable condition more quickly, suggesting greater ecological resilience.

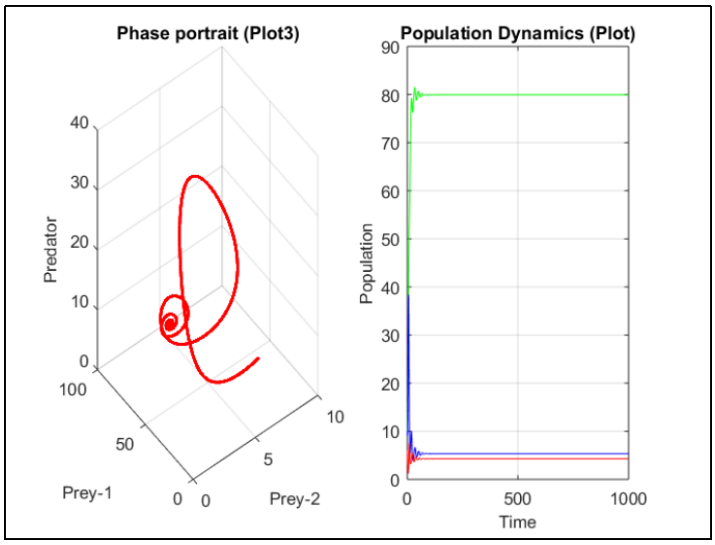

Figure 5. Phase portrait and time-series solution for $G = 0.50$.

In **Figure 6**, phase portrait and time-series solution depicting the coexistence equilibrium for $G = 0.70$ are depicted. Strong group defense significantly reduces effective predation, producing smaller oscillations and rapid convergence toward a stable coexistence equilibrium. This demonstrates that highly effective collective defense promotes long-term ecosystem stability and species persistence.

Figure 7 represents that a low predator mortality rate allows predators to persist for longer periods, resulting in stronger predator-prey interactions and larger oscillatory dynamics before coexistence is established.

Figure 8 shows that a moderate increase in predator mortality weakens predation pressure, reducing oscillation amplitudes and promoting a more balanced coexistence between predators and prey.

Figure 9 shows that as predator mortality increases, the predator population declines, and the prey can remain at higher densities without the system becoming unstable toward a stable coexistence equilibrium.

Figure 10 shows that a high mortality rate among large predators greatly suppresses predator persistence, leading to weak predator-prey interactions and dominance of prey populations. The results highlight the critical role of predator survival in maintaining ecological balance.

The parameter values used for the **Figures 3–10** are given in the following **Table 3**.

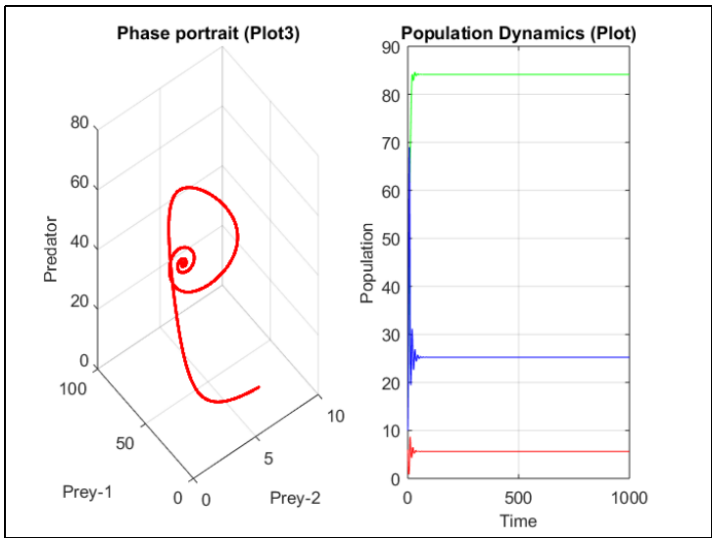

Figure 6. Phase portrait and time-series solution depicting the coexistence equilibrium for $G = 0.70$.

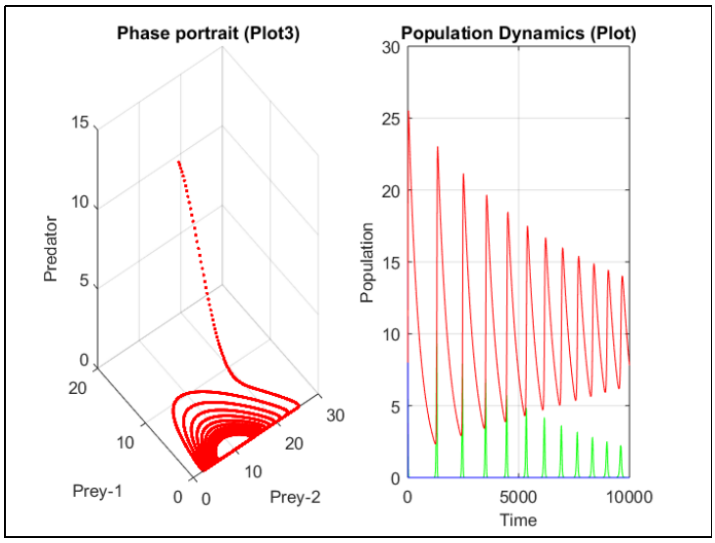

Figure 7. Phase portrait and time-series solution for $\delta = 0.002$.

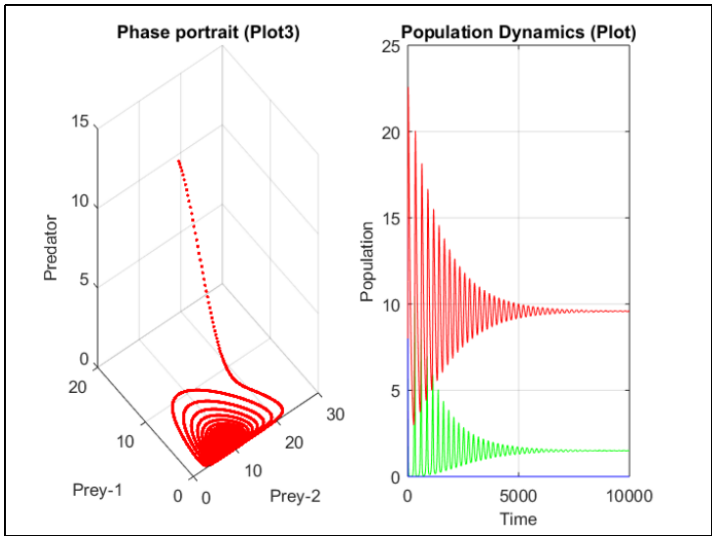

Figure 8. Phase portrait and time-series solution for $\delta = 0.009$.

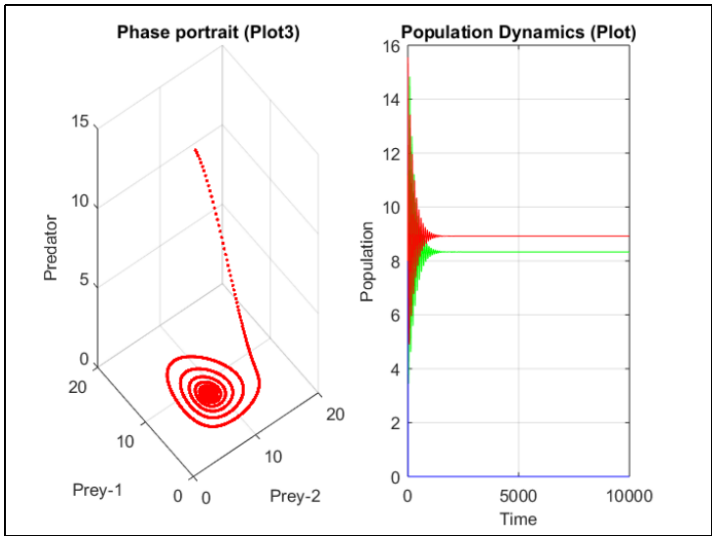

Figure 9. Phase portrait and time-series solution depicting the coexistence equilibrium for $\delta = 0.09$.

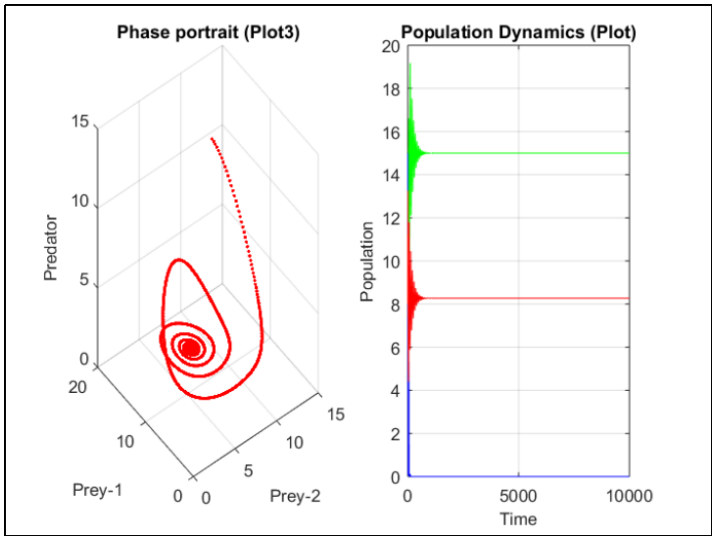

Figure 10. Phase portrait and time-series solution depicting the coexistence equilibrium for $\delta = 0.5$.

Table 3. Parameter values for the **Figures 3–10**.

Parameters Values	**Figures 3–6**	**Figures 7–10**
r_1	0.341	0.0934
r_2	0.697	0.697
K_1	100	100
K_2	100	100
α_1	0.032	0.032
α_2	0.3086	0.3086
β_1	0.020	0.020
β_2	0.060	0.060
δ	0.090	0.002, 0.009, 0.09, 0.5
G	0.1, 0.3, 0.5, 0.7	0.700
Initial Conditions	(10, 10, 6)	(10, 15, 8)

3.3. Parameter Selection and Sensitivity Analysis

The aim of this work is not to reproduce the behaviour of a real ecosystem but to consider the qualitative dynamics of an ecosystem influenced by the environment. The actual parameter values used in the numerical simulations are therefore representative biological parameters which are within typical ranges used in mathematical ecology. These are intended to represent the theoretical properties of the proposed model while remaining biologically realistic.

A local sensitivity analysis was performed to evaluate the robustness of the numerical results by varying one parameter at a time while holding the others at their original values. The values of each parameter were raised and lowered by 20%, and the equilibrium populations were calculated. The parameters chosen are the intrinsic growth rates of the prey r_1 and r_2, the attack rates of the predator α_1 and α_2, the mortality rate of the predator δ, the diffusion coefficient of the prey d_1, d_2, and the diffusion coefficient of the predator d_3, the environmental level of group-defense G.

The numerical experiments show that the group-defense parameter G has the strongest influence on the long-term population dynamics. Increasing G reduces the effective predation rate, resulting in higher prey densities and lower predator abundance. Conversely, increasing the predator attack rates α_1 and α_2 decreases prey populations while increasing predator density. Higher predator mortality δ reduces predator persistence and indirectly increases prey populations. Variations in the diffusion coefficients primarily affect the spatial distribution of the populations rather than their average densities. Finally, increasing the prey growth rates r_1 and r_2 leads to larger equilibrium prey populations and enhanced predator persistence through increased food availability.

Figure 11 presents the normalized local sensitivity in-

dices of the spatially averaged populations P, Q and N. Each parameter was varied independently by ±20%, while all remaining parameters were fixed at their baseline values. A positive sensitivity index indicates that an increase in the parameter increases the corresponding population, whereas a negative value indicates an inverse relationship.

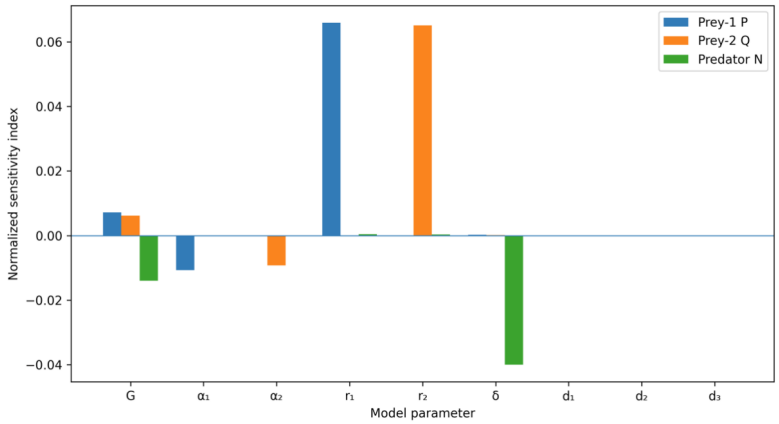

Figure 11. Normalized sensitivity of the mean prey and predator populations to ±20% variations in the principal model parameters at $T = 0.2$.

The prey-1 population P is most sensitive to its intrinsic growth rate r_1, followed by the predator attack rate α_1. Similarly, prey-2 Q is primarily influenced by its intrinsic growth rate r_2 and the attack rate α_2. Increasing r_1 or r_2 promotes prey growth, whereas increasing α_1 or α_2 reduces the corresponding prey population. The predator population N is most sensitive to the mortality rate δ and the group-defence level G. Both parameters have negative sensitivity indices, indicating that increased predator mortality or stronger prey group defence reduces predator abundance. The group-defense parameter simultaneously has positive effects on both prey populations because an increase in G decreases the effective predation factor, $1 - G$. The diffusion coefficients d_1, d_2, and d_3 exhibit relatively small sensitivity indices for the spatially averaged population densities over the considered simulation interval. This does not imply that diffusion is ecologically unimportant; rather, it mainly influences the spatial redistribution and smoothing of population profiles rather than strongly changing the total or mean population density.

Overall, the sensitivity analysis confirms that prey growth rates, predator attack rates, predator mortality, and group defense are the most influential parameters. The principal ecological conclusion remains robust: stronger group defense improves prey persistence and suppresses predator abundance.

4. Diffusive System

The spread of individuals through space (diffusion) is an important factor in predator-prey systems and can affect their complex dynamics and balance. This phenomenon results from multiple factors intrinsic to predator-prey relationships and environmental conditions. First, when essential resources, like food and suitable habitat, are distributed unevenly, individuals are driven to disperse in search of the best conditions, which creates unique spatial patterns in their distribution. Additionally, the geographic segregation of populations is facilitated by response-avoidance behaviours elicited by the presence of predators or decreased prey concentrations, and diffusion spreads these behaviours throughout the landscape.

The predator many factors that influence prey relationships. These factors significantly affect the habitat, which in turn shapes the population dynamics within it. In this section, we present the effects of species diffusion on the structural properties of the habitat. The diffusive version of the complex interaction among species arises because different species exhibit random movement in the habitat due to stimuli that attract or repel them. This movement may be towards or away from the other interacting species. The stimuli behind such movements may be food search, protection, etc. Here, we consider the self-diffusive predator-prey model to study the effects of diffusion on the population density of

interacting species. We assume $d_i, i = 1,\ 2,\ 3$ as diffusion coefficients. Consider,

$$\begin{gathered}\frac{\partial P}{dt} = d_1\nabla^2 P + r_1 P\left(1 - \frac{P}{K_1}\right)\\ -\alpha_1 PN\left(1 - \frac{G_{max}}{1+e^{-K(D-D_0)}}\right),\\ t > 0, x > 0\end{gathered} \tag{32}$$

$$\begin{gathered}\frac{\partial \mathrm{Q}}{\mathrm{dt}} = d_2\nabla^2 \mathrm{Q} + r_2 Q\left(1 - \frac{Q}{K_2}\right)\\ -\alpha_2 QN\left(1 - \frac{G_{max}}{1+e^{-K(D-D_0)}}\right),\\ t > 0, x > 0\end{gathered} \tag{33}$$

$$\begin{gathered}\frac{\partial \mathrm{N}}{\mathrm{dt}} = d_3\nabla^2 \mathrm{N} +\\ N\left(\beta_1 P + \beta_2 Q\right)\left(1 - \frac{G_{max}}{1+e^{-K(D-D_0)}}\right)\\ -\delta N, t > 0, x > 0\end{gathered} \tag{34}$$

with the following initial conditions

$$P(x,0) \geq 0, Q(x,0) \geq 0, N(x,0) \geq 0, x \in \Omega \tag{35}$$

and Neumann boundary conditions

$$\frac{\partial P}{\partial \nu} = \frac{\partial Q}{\partial \nu} = \frac{\partial N}{\partial \nu} = 0, x \in \partial\Omega.$$

The governing system consists of three coupled nonlinear reaction-diffusion equations describing the spatiotemporal evolution of the two prey populations, $P(x,t)$ and $Q(x,t)$, together with the predator population, $N(x,t)$. The diffusion terms $d_1\nabla^2 P$, $d_2\nabla^2 Q$, and $d_3\nabla^2 N$ represent random movement of individuals within the spatial domain, where $d_1,\ d_2$, and d_3 denote the corresponding diffusion coefficients. The logistic growth terms model density-dependent population growth limited by the carrying capacities K_1 and K_2. Predation terms describe predator-prey interactions, while the environmental group-defense function $G(D) = \frac{G_{max}}{1+e^{-K(D-D_0)}}$ reduces the effective predation rate according to the prevailing environmental conditions. Consequently, larger values of $G(D)$ correspond to stronger collective defence and lower predation efficiency.

System Stability at Equilibrium Point

For the stability of the system, we perturb (32)–(34) at the coexistence equilibrium point as under.

$$\frac{\partial P}{\partial t} = b_{11}P + b_{12}Q + b_{13}N + d_1\frac{\partial^2 P}{\partial x^2}, \tag{36}$$

$$\frac{\partial Q}{\partial t} = b_{21}P + b_{22}Q + b_{23}N + d_2\frac{\partial^2 Q}{\partial x^2}, \tag{37}$$

$$\frac{\partial N}{\partial t} = b_{31}P + b_{32}Q + b_{33}N + d_3\frac{\partial^2 N}{\partial x^2}. \tag{38}$$

Suppose the above system (36)–(38) possesses a Fourier solution.

$$\begin{cases} P(x,t) = \sum_K P_k e^{\lambda t} Cos(kx)\\ Q(x,t) = \sum_K Q_k e^{\lambda t} Cos(kx)\\ N(x,t) = \sum_K N_k e^{\lambda t} Cos(kx)\end{cases} \tag{39}$$

For $k = \frac{n\pi}{2}$, where n is a natural number, called the wave number at node n. By substituting the values of $P,\ Q, N$ in the above equations, we get the following.

$$\begin{cases} \lambda\sum_k P_k = b_{11}\sum_K P_k + b_{12}\sum_K Q_k\\ \quad +b_{13}\sum_K N_k - \sum_k P_k d_1 k^2\\ \lambda\sum_k Q_k = b_{21}\sum_K P_k + b_{22}\sum_K Q_k\\ \quad +b_{23}\sum_K N_k - \sum_k P_k d_2 k^2\\ \lambda\sum_k N_k = b_{31}\sum_K P_k + b_{32}\sum_K Q_k\\ \quad +b_{33}\sum_K N_k - \sum_k P_k d_3 k^2\end{cases} \tag{40}$$

This leads to the following result.

$$\begin{cases} \sum_K\left(b_{11} - \lambda - d_1k^2\right)P_k\\ +\sum_K b_{12}Q_k + \sum_K b_{13}N_k = 0\\ \sum_K b_{21}P_k + \sum_K\left(b_{22} - \lambda - d_2k^2\right)Q_k\\ +\sum_K b_{23}N_k = 0\\ \sum_K b_{31}P_k + \sum_K b_{32}Q_k +\\ \sum_K\left(b_{33} - \lambda - d_3k^2\right)N_k = 0\end{cases} \tag{41}$$

The dispersion relation is obtained from $det\ (V - \lambda I) = 0$, where the variational matrix V can be written as

$$V = \begin{bmatrix} b_{11} - d_1k^2 & b_{12} & b_{13}\\ b_{21} & b_{22} - d_2k^2 & b_{23}\\ b_{31} & b_{32} & b_{33} - d_3k^2\end{bmatrix}. \tag{42}$$

$$\begin{gathered}P(\lambda) = \lambda^3 + b_{13}b_{22}b_{31} - b_{12}b_{23}b_{31} - b_{13}b_{21}b_{32}\\ +b_{11}b_{23}b_{32} + b_{12}b_{21}b_{33} - b_{11}b_{22}b_{33} - k^2b_{23}b_{32}d_1\\ +k^2b_{22}b_{33}d_1 - k^2b_{13}b_{31}d_2 + k^2b_{11}b_{33}d_2 - k^4b_{33}d_1d_2\\ -k^2b_{12}b_{21}d_3 + k^2b_{11}b_{22}d_3 - k^4b_{22}d_1d_3 - k^4b_{11}d_2d_3\\ +k^6d_1d_2d_3 + \lambda^2\left(-b_{11} - b_{22} - b_{33} + k^2d_1 + k^2d_2 + k^2d_3\right)\\ +\lambda\left(-b_{12}b_{21} + b_{11}b_{22} - b_{13}b_{31} - b_{23}b_{32} + b_{11}b_{33}\right.\\ +b_{22}b_{33} - k^2b_{22}d_1 - k^2b_{33}d_1\\ -k^2b_{11}d_2 - k^2b_{33}d_2 + k^4d_1d_2\\ \left.-k^2b_{11}d_3 - k^2b_{22}d_3 + k^4d_1d_3 + k^4d_2d_3\right)\end{gathered}$$

The characteristic polynomial for the above matrix can be written as

$$P(\lambda) = \lambda^3 + S_1\lambda^2 + S_2\lambda + S_3 = 0. \tag{43}$$

Where,

$$S_1 = -b_{11} - b_{22} - b_{33} + k^2 d_1 + k^2 d_2 + k^2 d_3,$$

$$\begin{aligned} S_2 = &-b_{12}b_{21} + b_{11}b_{22} - b_{13}b_{31} - b_{23}b_{32} \\ &+b_{11}b_{33} + b_{22}b_{33} - k^2 b_{22}d_1 - k^2 b_{33}d_1 \\ &-k^2 b_{11}d_2 - k^2 b_{33}d_2 + k^4 d_1 d_2 - k^2 b_{11}d_3 \\ &-k^2 b_{22}d_3 + k^4 d_1 d_3 + k^4 d_2 d_3, \end{aligned}$$

$$\begin{aligned} S_3 = &b_{13}b_{22}b_{31} - b_{12}b_{23}b_{31} - b_{13}b_{21}b_{32} \\ &+b_{11}b_{23}b_{32} + b_{12}b_{21}b_{33} - b_{11}b_{22}b_{33} \\ &-k^2 b_{23}b_{32}d_1 + k^2 b_{22}b_{33}d_1 - k^2 b_{13}b_{31}d_2 \\ &+k^2 b_{11}b_{33}d_2 - k^4 b_{33}d_1 d_2 - k^2 b_{12}b_{21}d_3 \\ &+k^2 b_{11}b_{22}d_3 - k^4 b_{22}d_1 d_3 - k^4 b_{11}d_2 d_3 \\ &+k^6 d_1 d_2 d_3. \end{aligned}$$

According to Routh-Hurwitz's criterion, the system is stable under the following conditions.

$$S_1 > 0, S_3 > 0, S_1 S_2 > S_3. \tag{44}$$

To facilitate subsequent stability analysis, each equilibrium point corresponds to a biologically meaningful population state. The trivial equilibrium corresponds to complete extinction of all species. The boundary equilibria describe partial survival of one or more populations, and the coexistence equilibrium represents the simultaneous persistence of both prey species and the predator. The local stability analysis presented below determines whether small perturbations around these equilibrium states decay or amplify over time, thereby indicating the system's long-term ecological behaviour.

5. Construction of Numerical Scheme

The numerical approximation is constructed by discretizing both the temporal and spatial variables on a uniform computational grid. Time derivatives are approximated using the proposed three-level finite-difference formula, while second-order central finite differences are employed for the diffusion terms. At each time level, the nonlinear reaction terms are evaluated explicitly using the previously computed population values, allowing the complete coupled system to be advanced efficiently without solving nonlinear algebraic systems.

We have constructed an explicit scheme at three time levels. We use the following difference equation given under

$$\begin{aligned} u_i^{n+1} = &\tfrac{1}{5}\left(2u_i^n + 3u_i^{n-1}\right) \\ &+\Delta t\left\{a\left(\tfrac{\partial u}{\partial t}\right)_i^n + b\left(\tfrac{\partial u}{\partial t}\right)_i^{n-1}\right\}. \end{aligned} \tag{45}$$

The Taylor series expansion for, u_i^{n-1} and $\left(\frac{\partial u}{\partial t}\right)_i^{n-1}$ are given as

$$\begin{aligned} u_i^{n-1} = &u_i^n - \Delta t\left(\tfrac{\partial u}{\partial t}\right)_i^n + \tfrac{(\Delta t)^2}{2}\left(\tfrac{\partial^2 u}{\partial t^2}\right)_i^n \\ &-\tfrac{(\Delta t)^3}{6}\left(\tfrac{\partial^3 u}{\partial t^3}\right)_i^n + O\left((\Delta t)^4\right), \end{aligned} \tag{46}$$

$$\begin{aligned} \left(\tfrac{\partial u}{\partial t}\right)_i^{n-1} = &\left(\tfrac{\partial u}{\partial t}\right)_i^n - \Delta t\left(\tfrac{\partial^2 u}{\partial t^2}\right)_i^n \\ &+\tfrac{(\Delta t)^2}{2}\left(\tfrac{\partial^3 u}{\partial t^3}\right)_i^n + O\left((\Delta t)^3\right). \end{aligned} \tag{47}$$

We obtain the following by substituting Taylor series expansions (46)–(47) in Equation (45).

$$\begin{aligned} &u_i^n + \Delta t\left(\tfrac{\partial u}{\partial t}\right)_i^n + \tfrac{(\Delta t)^2}{2}\left(\tfrac{\partial^2 u}{\partial t^2}\right)_i^n \\ &+\tfrac{(\Delta t)^3}{6}\left(\tfrac{\partial^3 u}{\partial t^3}\right)_i^n + O\left((\Delta t)^4\right) = \\ &\tfrac{1}{5}\Big(2u_i^n + 3u_i^n - 3\Delta t\left(\tfrac{\partial u}{\partial t}\right)_i^n + 3\tfrac{(\Delta t)^2}{2}\left(\tfrac{\partial^2 u}{\partial t^2}\right)_i^n \\ &-\tfrac{(\Delta t)^3}{2}\left(\tfrac{\partial^3 u}{\partial t^3}\right)_i^n + O\left((\Delta t)^4\right)\Big) \\ &+\Delta t\left\{a\left(\tfrac{\partial u}{\partial t}\right)_i^n + b\left(\tfrac{\partial u}{\partial t}\right)_i^n - b\Delta t\left(\tfrac{\partial^2 u}{\partial t^2}\right)_i^n\right\}. \end{aligned} \tag{48}$$

Comparison of coefficients of $\Delta t\left(\frac{\partial u}{\partial t}\right)_i^n$, $(\Delta t)^2\left(\frac{\partial^2 u}{\partial t^2}\right)_i^n$ on both sides of Equation (48) leads to the following

$$1 = a + b - \frac{3}{5}, \tag{49}$$

$$\frac{1}{2} = \frac{3}{10} - b. \tag{50}$$

Solving the above Equations (49) and (50) gives the values of the unknown parameters a, b, are

$$a = \frac{9}{5},\ b = -\frac{1}{5}. \tag{51}$$

Hence, we get the following scheme by utilizing the unknowns in Equation (45)

$$u_i^{n+1} = \tfrac{1}{5}(2u_i^n + 3u_i^{n-1}) + \Delta t\left\{\tfrac{9}{5}\left(\tfrac{\partial u}{\partial t}\right)_i^n - \tfrac{1}{5}\left(\tfrac{\partial u}{\partial t}\right)_i^{n-1}\right\} \tag{52}$$

5.1. Stability Analysis of the Constructed Scheme

The purpose of the stability analysis is to determine whether small numerical or biological perturbations remain bounded as the solution evolves. This analysis complements the biological stability results by establishing numerical conditions under which the finite-difference approximation converges toward the true solution. The derived stability conditions therefore provide practical guidance for selecting

appropriate spatial and temporal discretization parameters in numerical simulations.

We use Von Neumann's stability criterion to discuss the stability of the numerical scheme. For this criterion, the difference equation obtained by applying a numerical scheme is transformed into another equation that contains the wave amplitudes and phase angles. Then, we apply the stability condition to the resulting equation, based on the ratio of wave amplitudes at different levels. We consider the following diffusive linear predator-prey model to discuss the stability of the scheme.

$$\frac{\partial u}{\partial t} = d_1 \frac{\partial^2 u}{\partial^2 x} + \overline{\alpha} u \tag{53}$$

The discretization using the presented scheme is given as

$$u_i^{n+1} = \tfrac{1}{5}(2u_i^n + 3u_i^{n-1}) + \Delta t \left\{ \tfrac{9}{5} \left(\tfrac{\partial u}{\partial t}\right)_i^n - \tfrac{1}{5} \left(\tfrac{\partial u}{\partial t}\right)_i^{n-1} \right\}.$$

Using the above equation for Equation (39)

$$\begin{gathered} u_i^{n+1} = \tfrac{1}{5}(2u_i^n + 3u_i^{n-1}) + \\ \Delta t \left\{ \begin{array}{c} ad_1 \left(\frac{u_{i+1}^n - 2u_i^n + u_{i-1}^n}{(\Delta x)^2} + \overline{\alpha} u_i^n \right) \\ + bd_1 \left(\frac{u_{i+1}^{n-1} - 2u_i^{n-1} + u_{i-1}^{n-1}}{(\Delta x)^2} + \overline{\alpha} u_i^{n-1} \right) \end{array} \right\} \end{gathered} \tag{54}$$

Consider the following transformations

$$\begin{gathered} u_i^{n+1} = E^{n+1} e^{iI\psi},\ u_{i\pm1}^n = E^n e^{(i\pm1)I\psi}, \\ u_{i\pm1}^{n-1} = E^{n-1} e^{(i\pm1)I\psi} \text{ where } I = \sqrt{-1} \end{gathered} \tag{55}$$

We substitute Equation (55) into Equation (54), and we obtain the following

$$\begin{gathered} E^{n+1} e^{iI\psi} = \tfrac{2}{5} E^n e^{iI\psi} + \tfrac{3}{5} E^{n-1} e^{iI\psi} + \\ \Delta t \left\{ \begin{array}{c} ad_1 \left(\frac{e^{(i+1)I\psi} - 2e^{iI\psi} + e^{(i-1)I\psi}}{(\Delta x)^2} \right) E^n + a\overline{\alpha} E^n e^{iI\psi} + \\ bd_1 \left(\frac{e^{(i+1)I\psi} - 2e^{iI\psi} + e^{(i-1)I\psi}}{(\Delta x)^2} \right) E^{n-1} + b\overline{\alpha} E^{n-1} e^{iI\psi} \end{array} \right\} \end{gathered} \tag{56}$$

Dividing both sides Equation (56) of by $e^{iI\psi}$ produces

$$\begin{gathered} E^{n+1} = \tfrac{2}{5} E^n + \tfrac{3}{5} E^{n-1} + \\ \Delta t \left\{ \begin{array}{c} ad_1 \left(\frac{e^{(i+1)I\psi} - 2e^{iI\psi} + e^{(i-1)I\psi}}{(\Delta x)^2} \right) E^n + a\overline{\alpha} E^n e^{iI\psi} + \\ bd_1 \left(\frac{e^{(i+1)I\psi} - 2e^{iI\psi} + e^{(i-1)I\psi}}{(\Delta x)^2} \right) E^{n-1} + b\overline{\alpha} E^{n-1} e^{iI\psi} \end{array} \right\}. \end{gathered}$$

$$\begin{gathered} E^{n+1} = \tfrac{2}{5} E^n + \tfrac{3}{5} E^{n-1} + \\ \Delta t \left\{ \begin{array}{c} ad_1 \left(\frac{2cos\psi - 2}{(\Delta x)^2} \right) E^n + a\overline{\alpha} E^n + \\ bd_1 \left(\frac{2cos\psi - 2}{(\Delta x)^2} \right) E^{n-1} + b\overline{\alpha} E^{n-1} \end{array} \right\}. \end{gathered} \tag{57}$$

Rewriting Equation (57), we get

$$\begin{gathered} E^{n+1} = \tfrac{2}{5} E^n + \tfrac{3}{5} E^{n-1} + \\ \left\{ \begin{array}{c} 2add_1(cos\psi - 1) E^n + a\ \Delta t \overline{\alpha} E^n + \\ 2bdd_1(cos\psi - 1) E^{n-1} + b\Delta t \overline{\alpha} E^{n-1} \end{array} \right\}. \end{gathered} \tag{58}$$

Where $d = \frac{\Delta t}{(\Delta x)^2}$.

Now, Equation (58) can be expressed as

$$E^{n+1} = PE^n + QE^{n-1}. \tag{59}$$

Where

$$\begin{gathered} (P = \tfrac{2}{5} + 2add_1(cos\psi - 1) + a\ \Delta t \overline{\alpha} \\ \text{and } Q = \tfrac{3}{5} + 2bdd_1(cos\psi - 1) + b\Delta t \overline{\alpha}. \end{gathered} \tag{60}$$

Since the presented numerical scheme is constructed on three time levels, one more equation is required to obtain an amplification matrix. An additional equation is expressed as

$$E^n = 1.E^n + 0.E^{n-1}.$$

The system of equations can be expressed in the following matrix-vector equation.

$$\begin{bmatrix} E^{n+1} \\ E^n \end{bmatrix} = \begin{bmatrix} P & Q \\ 1 & 0 \end{bmatrix} \begin{bmatrix} E^n \\ E^{n-1} \end{bmatrix}.$$

The amplification factor is a matrix, and the stability conditions can be imposed on the eigenvalues of the amplification matrix; these conditions are expressed as

$$\left| \frac{P + \sqrt{P^2 + 4Q}}{2} \right| \leq 1 \text{ and } \left| \frac{P - \sqrt{P^2 + 4Q}}{2} \right| \leq 1.$$

The scheme will be stable if it satisfies inequalities for positive eigenvalues of the amplification matrix, and if the eigenvalues of an amplification matrix are negative, then the stability condition is expressed as

$$|Q|^2 \leq 1.$$

Where the values of P & Q are presented in Equation (60).

5.2. Remark on Nonlinear Stability and Convergence

To verify the nonlinear performance of the proposed three-level scheme, numerical simulations are carried out for the diffusive predator-prey system. The following parameter values are used: $r_1 = 0.8$, $r_2 = 0.7$, $K_1 = 1.0$, $K_2 = 0.9$, $\alpha_1 = 0.35$, $\alpha_2 = 0.30$, $\beta_1 = 0.18$, $\beta_2 = 0.16$, $\delta = 0.20$, $d_1 = 0.005$, $d_2 = 0.004$, $d_3 = 0.003$. The computational domain is $0 \leq x \leq 1$ and the final time is $T = 0.2$. Homogeneous Neumann boundary conditions

are used. The initial conditions are taken as: $P(x,0) = 0.55 + 0.05\ \cos(\pi x)$, $Q(x,0) = 0.45 + 0.04\ \cos(2\pi x)$, $N(x,0) = 0.25 + 0.03\ \sin(\pi x)$. The first time level is generated by the explicit Euler method, and then the proposed three-level scheme is applied for $n \geq 1$.

Table 4 shows the numerical behaviour for different group-defense levels. The results show that increasing G reduces predation pressure. Therefore, the prey populations P and Q increase slightly, while the predator population N decreases.

Table 4. Effect of group defense on the numerical solution at $T = 0.2$.

G	**Mean *P***	**Mean *Q***	**Mean *N***
0.1	0.579592	0.475052	0.266685
0.4	0.582748	0.477285	0.263905
0.7	0.585887	0.479504	0.261139

The boundedness and positivity of the numerical solution are also verified. For $G = 0.4$, using $\Delta x = 0.01$ and $\Delta t = 2.5 \times 10^{-5}$, the following minimum and maximum values are obtained at $T = 0.2$.

Table 5 confirms that all computed population densities remain positive and bounded throughout the simulation.

Table 5. Positivity and boundedness of the computed solution for $G = 0.4$.

Variable	**Minimum Value**	**Maximum Value**
P	0.534977	0.630888
Q	0.438393	0.515301
N	0.247770	0.274389

To further verify the nonlinear convergence of the proposed method, mesh-refinement tests are performed in **Table 6**. The maximum norm error is calculated as: $Error = max_{\mathrm{i}} \left| u_{\mathrm{i}}(\Delta x,\ \Delta t) - u_{\mathrm{i}} \left(\frac{\Delta x}{2}, \frac{\Delta t}{2} \right) \right|$, where u represents P, Q, or N. The observed convergence rate is computed by: $Rate = \frac{\log\left(\frac{Error_1}{Error_2}\right)}{\log(2)}$. The recorded convergence rate is 2.1184.

The refinement study shows that the numerical error decreases as the grid is refined, confirming the scheme's stable, convergent behaviour for the nonlinear diffusive predator-prey system. These results complement the Von Neumann stability analysis and demonstrate that the proposed method is suitable for simulating nonlinear ecological dynamics that incorporate group defense and environmental effects.

Table 6. Mesh refinement study for the proposed scheme.

Grid Size	**Δt**	**Maximum Error**
51	1.0×10^{-4}	—
101	2.5×10^{-5}	8.9002×10^{-5}
201	6.25×10^{-6}	2.0497×10^{-5}

5.3. Numerical Simulations

We employ the constructed scheme on the diffusion model. The constructed scheme is given as under

$$u_i^{n+1} = \tfrac{1}{5}(2u_i^n + 3u_i^{n-1}) + \Delta t \left\{ \tfrac{9}{5} \left(\tfrac{\partial u}{\partial t} \right)_i^n - \tfrac{1}{5} \left(\tfrac{\partial u}{\partial t} \right)_i^{n-1} \right\}.$$

We get the following discretization using the constructed scheme for the first equation of the diffusive model (32)–(34).

$$P_i^{n+1} = \tfrac{1}{5}\left(2P_i^n + 3P_i^{n-1}\right) + \Delta t \left[\begin{array}{c} \tfrac{9}{5} \left\{ \begin{array}{c} d_1\left(P_{i+1}^n - 2P_i^n + P_{i-1}^n\right)/(\Delta x)^2 + \\ r_1 P_i^n \left(1 - \frac{P_i^n}{K_1}\right) - \\ \alpha_1 P_i^n N_i^n \left(1 - \frac{G_{max}}{1+e^{-K(D-D_0)}}\right) \end{array} \right\} \\ -\tfrac{1}{5} \left\{ \begin{array}{c} d_1\left(P_{i+1}^{n-1} - 2P_i^{n-1} + P_{i-1}^{n-1}\right)/(\Delta x)^2 + \\ r_1 P_i^{n-1} \left(1 - \frac{P_i^{n-1}}{K_1}\right) - \\ \alpha_1 P_i^{n-1} N_i^{n-1} \left(1 - \frac{G_{max}}{1+e^{-K(D-D_0)}}\right) \end{array} \right\} \end{array} \right]. \quad (61)$$

Similarly, we get

$$Q_i^{n+1} = \frac{1}{5}\left(2Q_i^n + 3Q_i^{n-1}\right) + \Delta t \left[\begin{array}{c} \frac{9}{5}\left\{ \begin{array}{c} d_2\left(Q_{i+1}^n - 2Q_i^n + Q_{i-1}^n\right)/(\Delta x)^2 + \\ r_2 Q_i^n\left(1 - \frac{Q_i^n}{K_2}\right) - \\ \alpha_2 Q_i^n N_i^n\left(1 - \frac{G_{max}}{1+e^{-K(D-D_0)}}\right) \end{array} \right\} \\ -\frac{1}{5}\left\{ \begin{array}{c} d_2\left(Q_{i+1}^{n-1} - 2Q_i^{n-1} + Q_{i-1}^{n-1}\right)/(\Delta x)^2 + \\ r_2 Q_i^{n-1}\left(1 - \frac{Q_i^{n-1}}{K_2}\right) - \\ \alpha_2 Q_i^{n-1} N_i^{n-1}\left(1 - \frac{G_{max}}{1+e^{-K(D-D_0)}}\right) \end{array} \right\} \end{array} \right], \quad (62)$$

$$N_i^{n+1} = \frac{1}{5}\left(2N_i^n + 3N_i^{n-1}\right) + \Delta t \left[\begin{array}{c} \frac{9}{5}\left\{ \begin{array}{c} d_3\left(N_{i+1}^n - 2N_i^n + N_{i-1}^n\right)/(\Delta x)^2 + \\ N_i^n\left(\beta_1 P_i^n + \beta_2 Q_i^n\right)\left(1 - \frac{G_{max}}{1+e^{-K(D-D_0)}}\right) \\ -\delta N_i^n \end{array} \right\} \\ -\frac{1}{5}\left\{ \begin{array}{c} d_3\left(N_{i+1}^{n-1} - 2N_i^{n-1} + N_{i-1}^{n-1}\right)/(\Delta x)^2 + \\ N_i^{n-1}\left(\beta_1 P_i^{n-1} + \beta_2 Q_i^{n-1}\right)\left(1 - \frac{G_{max}}{1+e^{-K(D-D_0)}}\right) \\ -\delta N_i^{n-1} \end{array} \right\} \end{array} \right]. \quad (63)$$

Equations (61)–(63) provide discretization based on the constructed scheme for the diffusive system.

Since the proposed method uses three-time levels, the solution at the first-time level must be computed before applying the main scheme. Let P_i^0, Q_i^0, and N_i^0 be obtained from the prescribed initial conditions. The first-time level is generated using the explicit Euler method as follows:

$$P_i^1 = P_i^0 + \Delta t \left[\begin{array}{c} \frac{d_1\left(P_{i+1}^0 - 2P_i^0 + P_{i-1}^0\right)}{(\Delta x)^2} \\ +r_1 P_i^0\left(1 - \frac{P_i^0}{K_1}\right) \\ -\alpha_1 P_i^0 N_i^0 (1 - G) \end{array} \right],$$

$$Q_i^1 = Q_i^0 + \Delta t \left[\begin{array}{c} \frac{d_2\left(Q_{i+1}^0 - 2Q_i^0 + Q_{i-1}^0\right)}{(\Delta x)^2} \\ +r_2 Q_i^0\left(1 - \frac{Q_i^0}{K_2}\right) \\ -\alpha_2 Q_i^0 N_i^0 (1 - G) \end{array} \right],$$

$$N_i^1\ N_i^0 + \Delta t \left[\begin{array}{c} \frac{d_3\left(N_{i+1}^0 - 2N_i^0 + N_{i-1}^0\right)}{(\Delta x)^2} \\ +N_i^0\left(\beta_1 P_i^0 + \beta_2 Q_i^0\right)(1 - G) \\ -\delta N_i^0 \end{array} \right].$$

After getting P_i^1, Q_i^1, and N_i^1, the proposed three-level scheme is applied for $n \geq 1$.

Figure 12 shows that spatial diffusion redistributes individuals throughout the habitat, reducing local population concentration and promoting more homogeneous species distributions.

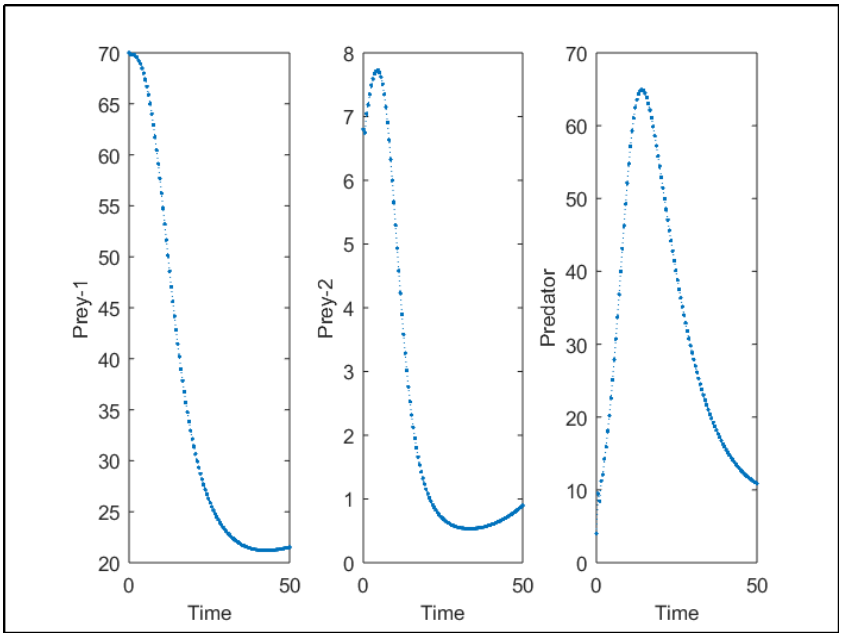

Figure 12. Numerical solution of the diffusive predator-prey system.

Figure 13 displays the impact of different initial conditions. The simulations show that diffusion can reduce sharp population gradients and prevent excessive fluctuations in the population level, leading to a more stable ecosystem in the spatial domain.

In **Figure 14**, the interaction between local population dynamics and diffusion promotes spatial persistence and prevents excessive aggregation, supporting long-term

coexistence of all species is depicted.

The trajectories in **Figure 15** show that coexistence is maintained at equilibrium and that spatial dispersal decreases the chances of the population fluctuations becoming unstable. Diffusion can thus be considered a stabilising ecological mechanism, as it distributes individuals over the habitat area.

The three-dimensional distributions in **Figure 16** show the temporal and spatial development of the ecosystem, and how the three functions of environmental regulation, group defence, and diffusion act together to regulate species abundance and sustain stable predator-prey coexistence across the habitat.

We present the numerical values of parameters taken for the **Figures 12–16** in **Table 7**.

Figure 17 depicts the impact of different time steps. It is clear from the figures that numerical method is convergent for different time steps.

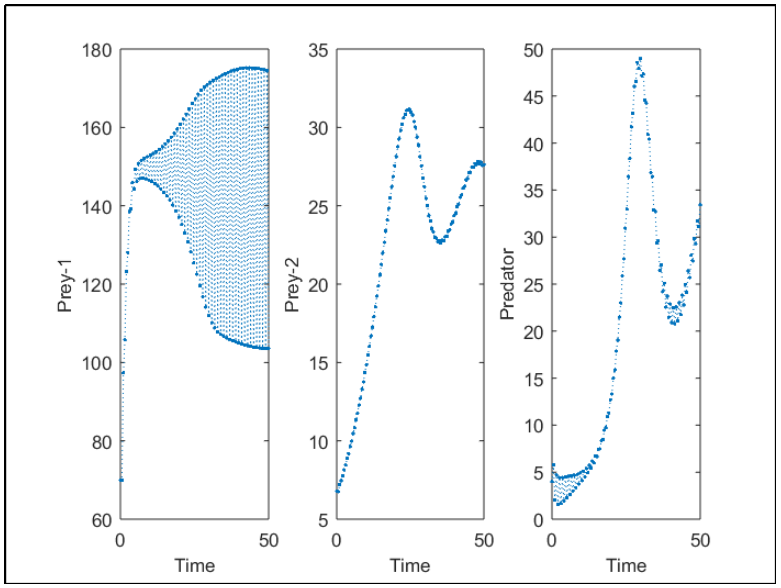

Figure 13. Results of the numerical solution of the diffusive predator-prey system under different spatial conditions.

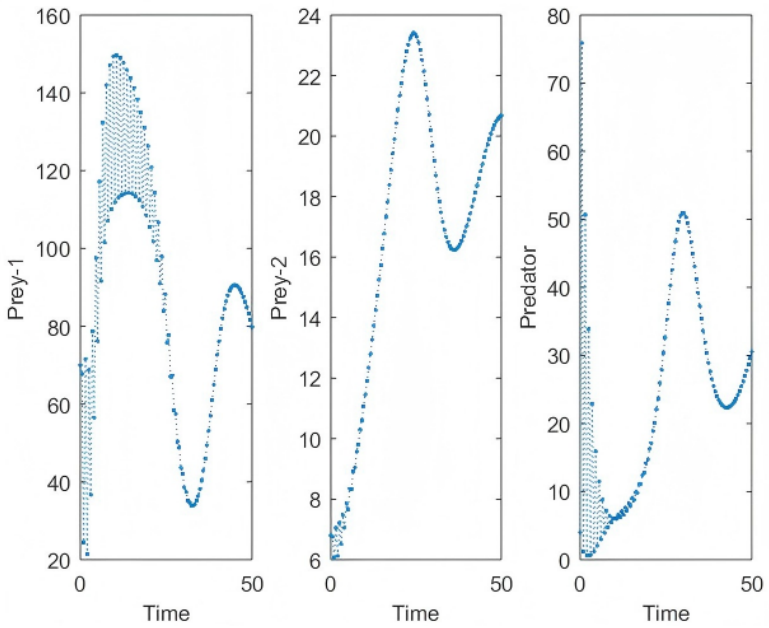

Figure 14. Numerical solutions of the diffusive predator-prey system showing the evolution of spatial population distributions.

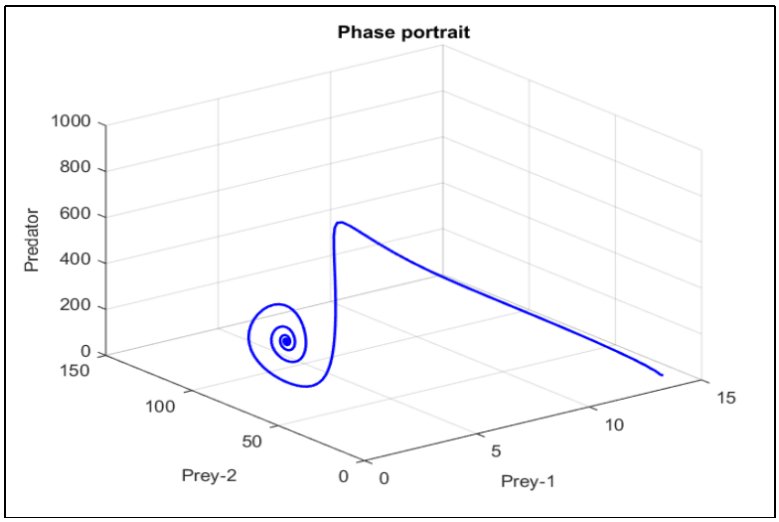

Figure 15. Phase portrait of the diffusive predator-prey system.

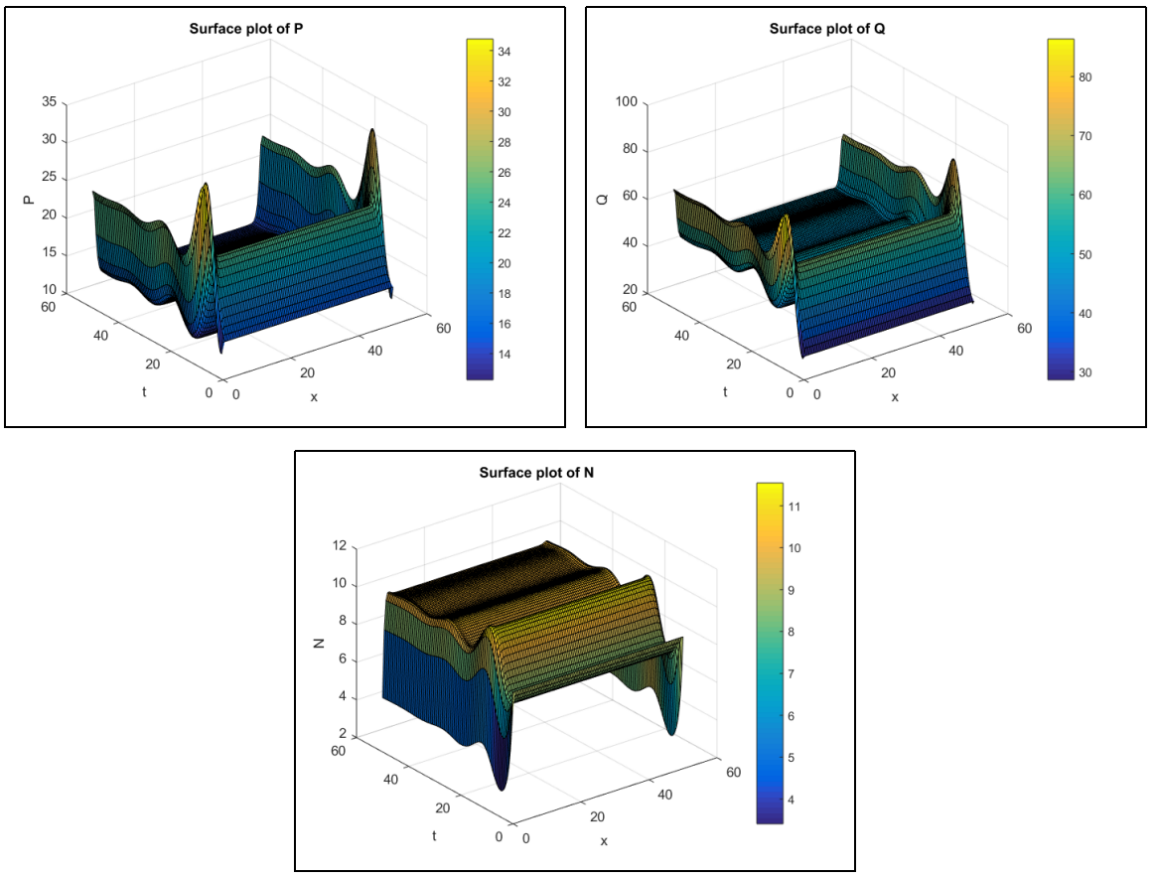

Figure 16. Surface plots of the interacting prey and predator populations.

Table 7. Numerical values of Parameters for **Figures 12–16**.

Parameters Values	Figure 12	Figure 13	Figure 14	Figure 15	Figure 16
r_1	0.0191	0.912	0.912	0.0532	0.9820
r_2	0.0949	0.097	0.097	0.9999	0.990
K_1	150	150	150	150	100
K_2	150	150	150	200	200

Table 7. *Cont.*

Parameters Values	Figure 12	Figure 13	Figure 14	Figure 15	Figure 16
α_1	0.0385	0.5081	0.5081	0.970	0.983
α_2	0.1348	0.0873	0.0873	0.1013	0.873
β_1	0.0214	0.014	0.014	0.896	0.020
β_2	0.0910	0.0191	0.0191	0.099	0.0432
δ	0.0948	0.948	0.6794	0.909	0.2002
G	0.9695	0.9695	0.9695	0.979	0.98
d_1	0.191	0.191	0.191	0.9191	0.081
d_2	0.06031	0.06031	0.06031	0.8706	0.071
d_3	0.0805	0.08051	0.08051	0.82088	0.090
Initial Conditions	(70, 6.8, 4)	(70, 6.8, 4)	(70, 6.8, 4)	(14, 10, 14)	(15, 30, 9)

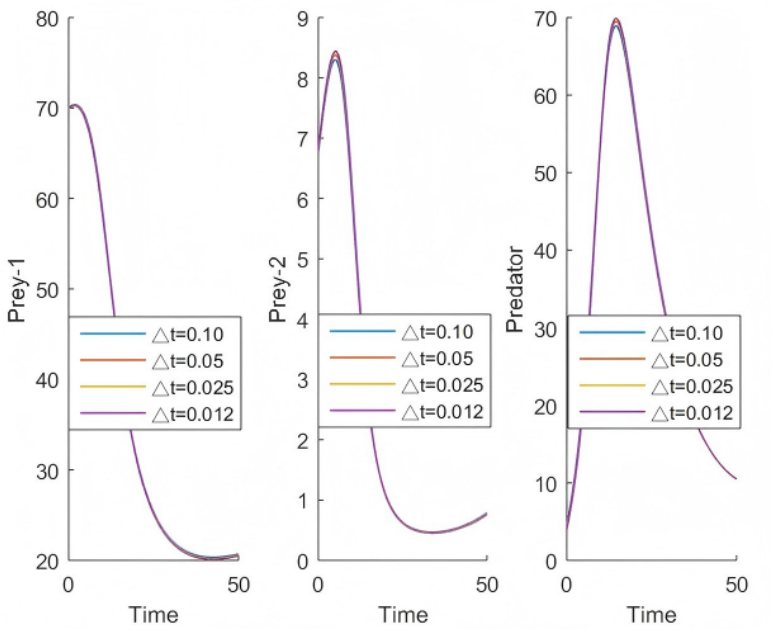

Figure 17. Plots with different time steps.

5.4. Quantitative Validation, Convergence, and Computational Efficiency

In **Table 8**, the temporal convergence results show that halving the time step reduces the maximum errors by approximately a factor of four for all population variables. The resulting orders observed range from 1.9868 to 2.0024, confirming second-order temporal accuracy.

The average observed temporal orders are approximately: P: 1.992, Q: 1.997, N: 2.001. Thus, the proposed method is second-order accurate in time.

In **Table 9**, the spatial-refinement experiment also produces convergence rates close to two. This agrees with the second-order central finite-difference approximation used for the diffusion terms. The convergence behaviour is consistent for prey-1, prey-2, and predator populations, demonstrating that the method does not lose its expected order when applied to the coupled nonlinear system.

Table 8. The spatial grid was fixed at $N_x = 401$. The benchmark was obtained using RK4 with $\Delta t = 0.003125$ on the same spatial grid.

Δt	E_∞ (P)	Order P	E_∞ (Q)	Order Q	E_∞ (N)	Order N	CPU (s)
0.5000	9.432×10^{-3}	—	2.4365×10^{-2}	—	3.7777×10^{-2}	—	0.0105
0.2500	2.380×10^{-3}	1.9868	6.107×10^{-3}	1.9963	9.429×10^{-3}	2.0024	0.0191
0.1250	5.98×10^{-4}	1.9926	1.529×10^{-3}	1.9974	2.356×10^{-3}	2.0005	0.0360
0.0625	1.50×10^{-4}	1.9961	3.83×10^{-4}	1.9985	5.89×10^{-4}	2.0000	0.0748

Table 9. Spatial refinement study and convergence order.

N_x	Δx	E_∞ (P)	Order	E_∞ (Q)	Order	E_∞ (N)	Order	CPU (s)
51	20	4.41×10^{-4}	—	3.91×10^{-4}	—	1.515×10^{-4}	—	1.0384
101	10	1.11×10^{-4}	1.9873	9.90×10^{-5}	1.9889	3.965×10^{-5}	1.9339	1.1019
201	5	2.80×10^{-5}	2.0128	2.50×10^{-5}	1.9990	9.874×10^{-6}	2.0054	1.2067
401	2.5	7.0×10^{-6}	2.0693	6.0×10^{-6}	2.0694	2.361×10^{-6}	2.0645	1.3861
801	1.25	1.0×10^{-6}	2.3217	1.0×10^{-6}	2.3214	4.722×10^{-7}	2.3216	1.7596

The time step was fixed at $\Delta t = 0.003125$. A reference solution was computed using the same three-level method on $N_x = 1,601$ spatial points so that temporal error was common to all comparisons and the measured error primarily represented spatial discretization.

The rates are close to two over the principal refinement range, confirming the expected second-order accuracy of the central spatial difference approximation. The higher final rates occur because the solutions approach the refined-grid reference and the errors become very small.

In **Table 10**, the proposed method and the RK4-central difference method produce closely agreeing numerical solutions. As expected, RK4 yields lower errors at the same time step because it is fourth-order accurate in time. Nevertheless, the proposed scheme requires only one new evaluation of the nonlinear reaction-diffusion operator per time step after initialization, while RK4 requires four. The measured CPU time was approximately 0.0581 s for the proposed method and 0.1977 s for RK4, corresponding to a computational speed-up of approximately 3.4.

Table 10. The comparison was performed on $N_x = 201$ with $\Delta t = 0.0625$ and $T = 50$. CPU times are median values from three runs in the same execution environment.

Method	$E_\infty(P)$	$E_\infty(Q)$	$E_\infty(N)$	$E_2(P)$	$E_2(Q)$	$E_2(N)$	CPU (s)
Proposed three-level scheme	1.41×10^{-4}	4.00×10^{-4}	5.91×10^{-4}	2.693×10^{-3}	1.035×10^{-2}	1.798×10^{-2}	0.0581
RK4-central difference	2.60×10^{-5}	2.30×10^{-5}	9.00×10^{-6}	4.50×10^{-4}	3.89×10^{-4}	1.26×10^{-4}	0.1977

RK4 is more accurate at the same time-step size because it is fourth order in time. However, the proposed method is approximately: CPU speed-up = $0.1977/0.0581 \approx 3.40$. Therefore, at this grid and time step, the proposed method is about 3.4 times faster and requires only one new nonlinear operator evaluation per time level, compared with four operators for RK4.

6. Results and Discussion

We investigate the population dynamics of interacting species across a series of figures, exploring the effects of different parameters. These numbers give insight into how changes in parameters affect prey and predator in an ecological system. **Figures 1** and **2** show how the prey's group defense is affected by the driving factor. At $D = 0$, G is minimal, likely around 0.6. As D increases, G will also increase rapidly at first because of the exponential term, ultimately peaking at $G = 1$ at $D = 8$. Once D has passed the point at which G has its peak value, the curve levels off to show that increases in D have little effect on G and that G continues to be its maximum value $G = 1$. This function is a case in which the group defense of prey species will rise quickly as the driving factor D rises initially and then level off when D is increased further. In an ecological sense, this would be the case if prey species respond to a threat by becoming more adept at defending themselves until, at a certain point, further improvement in their defence yields no additional benefit.

The plotted curves in **Figure 2** depict the relationship between the driving factor D and the group defensce offered by prey species, with each curve exhibiting inflexion points at $D = 2$, $D = 4$, and $D = 6$. Notably, the curve corresponding to the inflection point at $D = 2$ starts defense offerings at a very low value, around 0.02, and quickly escalates to its maximum value of 1, achieving this earlier than the other curves due to the earlier inflection point. Conversely, the curves associated with inflection points at $D = 4$ and $D = 6$ initiate defense from $G = 0$ and exhibit gradual increases until they reach their respective inflection points. Following these points, the rate of defense elevation accelerates, resulting in steeper slopes around $D = 4$ and $D = 6$. Ultimately, all curves attain the same maximum defence value

of 1; however, the timing of this attainment depends on the positions of the inflexion points. This portrayal illustrates how different inflexion points can influence the trajectory and pace of the prey species' defense response to the driving factor, thereby depicting nuanced dynamics in ecological or evolutionary scenarios.

The location and direction of the inflexion points in the curves denote critical thresholds at which the defense value of the prey species changes its rate of increase or decrease, and therefore are points of added sensitivity or adaptation to environmental pressures. When inflection points are lower on the D value, the more rapid the escalation of defense strategies, which can help to counter threats earlier. Other species, however, with inflection points at higher D values, might need stronger environmental signals to trigger strong defense mechanisms. The knowledge gained from these dynamics can help elucidate how prey species adapt to environmental changes, enhancing understanding of the ecosystem.

The effect of the parameter *G* (group defense) on populations of the interacting species is explored in **Figures 3–6**. The plots on the left show phase portraits, and those on the right show time-series solutions; both are used to assess the stability of the equilibrium points in the predator-prey system. The time-series solutions are coloured: green for prey-1, blue for prey-2, and red for predators. In the phase portraits, the trajectories of the system are shown in red. An examination of the time series shows that as the level of the defense mechanism, G, increases, the populations of both prey species increase. Considering the paths of the prey-1 (green) states, we can see that the stabilization points move with the increasing value of G. Specifically, for $G = 0.1$, prey-1 stabilizes at 53; for $G = 0.3$, it stabilizes at 68; for $G = 0.5$, it stablizes at 80; and for $G = 0.7$, it stabilizes at 84. This suggests that the larger the value of *G*, the larger the stabilised prey-1 population. This correlation emphasises the importance of predator-prey interactions in maintaining prey population equilibrium in predator-prey systems through defence mechanisms. These insights are supported by the phase portraits, which show the trajectory of the system and highlight the dynamics and stability of the equilibrium points as a function of G. Overall, these plots provide valuable visualizations of how changes in defence mechanisms affect the dynamics and stability of predator-prey populations. The initial conditions for these simulations are set at (10, 10, 6), denoting the initial populations of prey-1, prey-2, and predators, respectively. As group defence strength increases, prey become more resistant to predator attacks, leading to noticeable changes in the system's long-term population dynamics. The gradual increase in group defense shifts the system from a regime dominated by competitive exclusion toward one that supports greater species persistence and coexistence, demonstrating the stabilizing role of collective defense in maintaining ecological balance. **Figures 3** and **4** depict the classical phenomenon of competitive exclusion over the shorter simulation period ($t = 1,000$). In these cases, prey-1 disappears quickly during the early stage of the simulation ($t < 50$), leaving prey-2 and the predator in the ecological system. It is clear from these plots that, after a few initial oscillations, the two populations gradually settle into a stable equilibrium, indicating that the ecosystem reaches a balanced predator–prey relationship once the weaker prey species has vanished.

Figures 5 and **6** show a different ecological outcome in which coexistence of all three species is obvious. With these parameter settings, prey-1 can persist rather than go extinct, allowing both prey species to coexist with the predator. **Figure 4** shows that the equilibrium densities of both prey species are noticeably higher, suggesting more favourable environmental conditions. At the same time, the predator continues to regulate the prey populations and sustain the overall stability of the system.

In **Figures 6–10**, we investigate the influence of δ, which represents the predator's death rate, on the ecological system. Like the previous figures, an increase in δ results in reduced predation, leading to an upsurge in prey populations, especially prey-1. The same colour scheme is used, with green representing prey-1, blue for prey-2, and red for predators. The initial conditions for these simulations are set at (10, 15, 8). **Figures 7** and **8** demonstrate the influence of the predator mortality rate, δ, on the long-term population dynamics over the extended simulation period ($t = 10,000$). The predator death rate is increased in steps from δ = 0.002 to 0.009, 0.09, and 0.50. As δ increases, predator survival becomes progressively more difficult, altering the balance between predation pressure and prey growth. Consequently, the system exhibits noticeable changes in transient behavior, oscillation patterns, and equilibrium population densities, il-

lustrating the important role of predator mortality in shaping ecosystem stability and species persistence.

When the simulation is extended to 10,000, the long-term behaviour becomes more evident. **Figure 7** shows that Prey-1 again goes to extinction very early in the simulation. However, the remaining predator/Prey-2 system experiences large population fluctuations for a long time before eventually approaching a stable state. These oscillations reflect the repeated rise and fall of prey and predator populations as they gradually move toward equilibrium.

Figures 8–10 illustrate increasingly stable long-term dynamics. In **Figure 8**, the predator continues to exert strong control over the prey population, leading to prolonged oscillations before the system stabilises. **Figure 9** reaches equilibrium more rapidly, with the oscillations dying out fastly, indicating a stronger stabilizing effect. **Figure 8** shows the most stable scenario, where a relatively large Prey-2 population supports the predator while preventing large fluctuations, resulting in a well-balanced, resilient ecosystem over the long term.

Figure 11 shows the system's overall balance that comes down to a few straightforward drivers: each prey population's size is devastatingly powered by its own internal growth rate (r_1,r_2), whereas the predator population is most sensitive to its own mortality rate, taking a sharp hit whenever death rates increase. Elevated attack rates (α_1, α_2) naturally trim down prey numbers, and raising general habitat capacity (G) helps both prey species while surprisingly causing a small dip in predator numbers due to top-down feedback loops. Lastly, the diffusion terms ($d_1,\ d_2, d_3$) sit right at zero, proving that how quickly or slowly species move across space has virtually no effect on their long-term average population densities.

Figures 12–14 are dedicated to the analysis of a diffusion system. These plots, which are drawn for different values of G (0.1, 0.3, 0.5, 0.7), provide insights into the system's behaviour. The initial conditions for these simulations are (70, 6.4, 4).

The oscillatory behaviour observed in **Figures 12–14**, which depicts the solution of a diffusive system for the selected parameters, can be attributed to the interplay between diffusion and reaction processes within the ecological system. Diffusion, representing the movement of individuals across space, can lead to spatial heterogeneity in population densities. Meanwhile, processes such as predation and reproduction affect population dynamics. In diffusive systems, these processes are coupled, leading to oscillations in response to spatial variability and feedback processes. Oscillatory behaviour arises from the system's intrinsic dynamics, in which fluctuations in population densities propagate spatially and temporally, resulting in periodic patterns. These oscillations may reflect underlying instabilities or feedback loops within the ecosystem, highlighting the complex dynamics inherent in ecological systems. Understanding the technical details of diffusion and reaction processes, as well as their combined effects, is essential for elucidating the observed oscillatory behaviour and its implications for ecosystem dynamics and stability. **Figure 15** illustrates the phase portrait of the diffusive system. This portrait helps us understand the stability of a coexistence fixed point within the system.

The initial conditions for this specific plot are (14, 10, 14). The parameter values for all **Figures 3–16** are given in **Tables 3** and **7**. The observed surface plot depicts the spatial distribution of predator (Q) populations over time, with the spatial axis (x) representing different spatial coordinates, the temporal axis (y) representing time, and the population axis (z) indicating predator density. **Figure 16** displays surface plots that illustrate the spatial and temporal impacts on the interacting population. Observing the plots, we observed the variation in population. For instance, in the prey-2 plots, we found that at a fixed time point (t = 8.586), the surface plot provides a valuable understanding of the spatial dynamics of predator populations. Despite varying spatial coordinates along the x-axis, the population of prey-2 remains relatively constant. Specifically, for spatial coordinates ranging from 2.525 to 20.2, the predator population remains around 56 individuals, exhibiting minimal variation. However, at a spatial coordinate of 48.99, the predator population notably increases to 70.47 individuals. The consistent prey population across most spatial coordinates implies spatial homogeneity in predator distribution at this point. The slight increase in predator population at a specific spatial coordinate (x = 48.99) suggests localized variations in habitat conditions. Despite spatial variations, the overall stability of predator populations over time suggests a level of resilience or equilibrium in predator-prey dynamics within the ecosystem. This stability may arise from regulatory mechanisms such as predator-prey interactions, density-dependent pro-

cesses, or environmental feedback loops.

The proposed model also matches previous theoretical studies of predator-prey systems. Previous research has shown that group-defence mechanisms decrease predator attack efficiency and increase prey persistence, and reaction-diffusion models have shown that spatial dispersal allows coexistence and spatially stable population distributions. The current study builds on this previous research. It presents a unified mathematical model that combines environmentally regulated group defence, two-prey-one-predator dynamics, reaction-diffusion processes, rigorous analytical stability analysis, and a new numerical model comprising three levels. While previous formulations assumed constant defense intensity, the proposed formulation allows collective defense to be flexible and continuously adjusted to environmental conditions, making it more realistic for representing ecological systems affected by environmental variability, resource levels, and habitat quality.

To further verify the numerical performance of the proposed three-level finite difference scheme, additional simulations were carried out using different time-step sizes while keeping all model parameters and initial conditions unchanged. The numerical solutions obtained for different values of Δt exhibit consistent qualitative behaviour, indicating that the proposed numerical method produces stable and reliable approximations over the considered range of discretisation parameters. These results provide numerical support for the theoretical Von Neumann stability analysis and confirm the robustness of the proposed scheme for solving the nonlinear predator-prey system (see **Figure 17**).

The results of the analysis and calculations are generally consistent, showing that the interaction between environmental quality, prey defensive behaviour, and spatial dispersion governs ecosystem stability. Collective defense is enhanced by environmental improvement, spatial persistence by diffusion, and ecosystem resilience and decreased risk of population collapse by both. The results advance our understanding of predator-prey dynamics regulated by the environment and offer a flexible mathematical model for future studies on stochastic environments, habitat fragmentation, seasonal variations, and adaptive predator-prey behavioural responses.

7. Conclusions

Our investigation into the mechanisms that guide group defense in a three-species model has provided insights into the complex dynamics of predator-prey interactions. By identifying equilibrium points, analyzing system stability through Lyapunov functions, and examining stability using the Routh-Hurwitz criterion, we have gained a nuanced understanding of the patterns within this ecological system. In the present research, a three-species predator-prey model is formulated that accounts for prey species group defense. The positivity and boundedness of the solution is discussed. The model's equilibrium points are computed, and the coexistence equilibrium points are analysed for local and global stability. Moreover, the diffusive version of the model is presented. The stability of the diffusive version is also presented. An explicit numerical scheme is presented and analysed using the Von Neumann method. It is concluded that the coexistence model shows local and global stability under some conditions. Group defense in prey species reduces the risk of predation. As we enhance the value of G, the prey population rises due to a reduced attack rate. The predator's death rate significantly affects the population dynamics of interacting species. An increase in the death rate enhances the prey population. The diffusive version of the model is presented to see the impact of diffusion. A numerical scheme is constructed, and it is concluded that it is conditionally stable. The solution of the diffusive system is presented using the constructed scheme. The phase portrait illustrates the stability of the diffusive system and demonstrates the coexistence of the interacting populations under the assumed parameter values.

We found that resource availability and habitat quality are key factors in the dynamics of these systems and should be considered. Adding the group defense mechanisms of both prey species adds another dimension to understanding the phenomenon. It illustrates the relationship between environmental factors and strategies used by the species in the ecosystem. This study is useful in the field of ecology and is significant for ecological issues of biodiversity management and conservation. In this way, we begin to understand the dynamics and stability of species ecosystems in which group defense is involved, paving the way for more informed ecological management, particularly in the context of diffusion.

The model is proposed and shown to play a funda-

mental role in explaining the persistence and coexistence of interacting species, depending on environmental conditions and their group-defense strategies. Analytical and numerical analyses indicate that the strength of collective defense is an important factor in long-term predator distribution, lowering predation pressure and increasing prey survival. Spatial diffusion also helps stabilise population distribution by enabling species to spread and exploit resources more efficiently.

The results of this study have ecological implications for wildlife management and ecosystem conservation. The model proposes that if prey species can maintain resources and habitat in a state that supports high habitat quality, their natural defense behaviours will be reinforced, leading to greater biodiversity and reduced risk of local extinction. The outcomes could also be useful for conservation practitioners in designing nature reserves, enhancing habitat connectivity, and assessing biological control programmes, particularly when predator-prey relationships are important in shaping population dynamics within an ecosystem. Additionally, the proposed framework can be extended to explore the implications of climate change, habitat fragmentation, invasive species, and adaptive management policies on ecological stability. The additional extensions are promising areas for future research and enhance the usefulness of the proposed mathematical model.

Our research is relevant and contributes to the field by providing an approach to modelling and studying complex systems. It has emphasized mechanisms that influence the long-term viability and adaptability of ecosystems in response to changes. As fractional calculus is a valuable tool for modeling natural phenomena, we shall extend the model to its fractional version in the future.

In the present study, we showed that these two processes, group defense and spatial diffusion, are essential mechanisms for predator-prey coexistence and ecosystem stability, and that they are regulated by environmental factors. In addition to establishing the model's mathematical properties and designing an effective numerical tool, the proposed model provides ecological insights for biodiversity conservation, habitat restoration, wildlife management, and biological control. The findings indicate that enhancing habitat quality and habitat connectivity can boost the effectiveness of natural collective defense mechanisms, species persistence, and ecosystem resilience to environmental disturbance. The proposed framework is therefore a valuable mathematical tool for exploring conservation strategies and assessing potential future climate variability, habitat fragmentation, and ecological consequences.

7.1. Limitations

The present model has several limitations: it investigates predator-prey interactions with environmentally induced group defense and spatial diffusion, but it is unclear how these features influence the dynamics of the entire system. Natural ecosystems are affected by seasonal variations, environmental uncertainty, habitat fragmentation, and demographic stochasticity, which are not included in the current formulation. Furthermore, the model has not been applied to field observations and may therefore have limited direct application to certain ecological systems.

The framework presented here, although limited, offers a valuable mathematical tool for exploring the impact of environmental conditions on the coexistence of predators and prey and on the stability of the ecosystem. The findings may have implications for biodiversity conservation, wildlife management, ecological risk assessment and ecosystem rehabilitation, particularly in situations where predator-prey relationships are heavily influenced by collective prey.

7.2. Future Directions

Future work will investigate the impact of stochastic environmental fluctuations on the model, the importance of spatially heterogeneous habitats, the inclusion of seasonality, adaptive dispersal mechanisms and other ecological interactions such as competition, disease transmission and age/stage structure. Another part will estimate the model parameters using ecological observations and validate the proposed framework using empirical data. This will improve the realism of the model and extend its utility for real-world ecological management and conservation challenges.

Author Contributions

Conceptualization, M.S.A. and A.E.; methodology, A.E.; software, A.E.; validation, M.S.A. and A.E.; formal analysis, M.S.A.; investigation, A.E.; resources, M.S.A.; data curation, A.E.; writing—original draft preparation,

M.S.A.; writing—review and editing, A.E.; visualization, M.S.A.; supervision, M.S.A.; project administration, M.S.A.; funding acquisition, M.S.A. All authors have read and agreed to the published version of the manuscript.

Funding

This research did not receive any specific grant from public, commercial, or not-for-profit funding agencies.

Institutional Review Board Statement

Not applicable.

Informed Consent Statement

Not applicable.

Data Availability Statement

The manuscript included all required data and the implementation of information.

Acknowledgments

The authors wish to express their gratitude to Prince Sultan University for facilitating the publication of this article through the Theoretical and Applied Sciences Lab.

Conflicts of Interest

The authors declare no conflict of interest.

AI Use Statement

No AI tools were used for data analysis, interpretation, or generation of scientific content. All outputs were critically reviewed and edited by the authors. The authors take full responsibility for the integrity and accuracy of the work.

References

[1] Murray, J.D., 2002. Mathematical Biology I: An Introduction, 3rd ed. Springer: New York, NY, USA.

[2] Meron, E., 2015. Nonlinear Physics of Ecosystems. CRC Press: Boca Raton, FL, USA.

[3] Ermentrout, G.B., Rinzel, J., 1981. Waves in a simple, excitable or oscillatory, reaction-diffusion model. Journal of Mathematical Biology. 11(3), 269–294.

[4] Kazantsev, V., Nekorkin, V., Binczak, S., et al., 2003. Spiking patterns emerging from wave instabilities in a one-dimensional neural lattice. Physical Review E. 68(1), 017201.

[5] Sevcikova, H., Marek, M., 1991. Wave patterns in an excitable reaction-diffusion system. Physica D: Nonlinear Phenomena. 49(1–2), 114–124.

[6] Du, N.H., Nguyen, N.N., 2025. Analysis of reaction-diffusion predator-prey system under random switching. Nonlinear Analysis: Hybrid Systems. 58, 101621.

[7] Fan, X., Zhang, W., Xu, L., 2025. Global dynamics of a predator-prey model with prey-taxis and hunting cooperation. Electronic Research Archive. 33(3), 1610–1632.

[8] Jia, L., Wang, C., 2025. Stability analysis of a four-species periodic diffusive predator-prey system with delay and feedback control. Biology. 14(5), 462.

[9] Ko, W., Ryu, K., 2025. A diffusive predator-prey system with hunting cooperation in predators and prey-taxis: I. Global existence and stability. Journal of Mathematical Analysis and Applications. 543(2), 129005.

[10] Lam, K.-Y., Lee, R., 2024. Asymptotic spreading of predator-prey populations in a shifting environment. Mathematics in Applied Sciences and Engineering. 5(3), 199–221.

[11] Lou, Y., Tao, W., Wang, Z.-A., 2025. Effects and biological consequences of the predator-mediated apparent competition II: PDE models. Journal of Mathematical Biology. 91(5), 55.

[12] Qi, H., Jin, J., Liu, B., et al., 2025. Stationary distribution of a stochastic reaction-diffusion predator-prey model with additional food, fear effect and anti-predator behavior. Applied Mathematics Letters. 169, 109612.

[13] Tao, W., Wang, Z.-A., 2025. Global well-posedness and Turing-Hopf bifurcation of prey-taxis systems with hunting cooperation. European Journal of Applied Mathematics. in Press.

[14] Yu, H., Yang, W., Li, Y., 2025. Effects of anisotropic diffusion on the dynamics of a predatorprey system in heterogeneous environments. Discrete and Continuous Dynamical Systems - B. 30(1), 265–288.

[15] Zhang, Y., Jiang, T., Wang, C., et al., 2025. Stability analysis of a nonautonomous diffusive predator-prey model with disease in the prey and Beddington-DeAngelis functional response. Biology. 14(12), 1779.

[16] Akhtar, P., Santra, N., Samanta, G., 2026. Study on fear-induced group defense and cooperative hunting: bifurcation, uncertainty, seasonality, and spatio-temporal analysis in predator-prey system. The European Physical Journal Special Topics. 1–40.

[17] Bhargava, M., Dubey, B., 2025. Bifurcation analysis

and Turing pattern formation on multiplex networks of ecological model with trade-off dynamics. The European Physical Journal Plus. 140(10), 1001.

[18] Singh, A., Kumar, A., Gupta, A., et al., 2025. Bifurcation and chaos in a diffusive prey-predator model incorporating fear effect on prey and team hunting by predator with anti-predation response delay. International Journal of Bifurcation and Chaos. 35(2), 2550018.

[19] Pal, S., Karmakar, S., Pal, S., et al., 2024. Impact of fear and group defense on the dynamics of a predator-prey system. International Journal of Bifurcation and Chaos. 34(2), 2450019.

[20] Kim, S., Antwi-Fordjour, K., 2022. Prey group defense to predator aggregated induced fear. The European Physical Journal Plus. 137(6), 704.

[21] Roy, J., Dey, S., Kooi, B.W., et al., 2024. Prey group defense and hunting cooperation among generalist-predators induce complex dynamics: A mathematical study. Journal of Mathematical Biology. 89(2), 22.

[22] Mimura, M., Nagayama, M., 1997. Nonannihilation dynamics in an exothermic reaction-diffusion system with mono-stable excitability. Chaos. 7(4), 817–826.

[23] Roy, S., Byrne, H.M., Banerjee, J., et al., 2025. Spatio-temporal eco-evolutionary dynamics of prey-predator systems with defended and undefended prey. Communications Physics. 9(1), 4.

[24] Zemskov, E.P., Tsyganov, M.A., Horsthemke, W., 2017. Oscillatory pulses and wave trains in a bistable reaction-diffusion system with cross diffusion. Physical Review E. 95(1), 12203.

[25] Roussel, M.R., Wang, J., 2004. Pattern formation in excitable media with concentration-dependent diffusivities. The Journal of Chemical Physics. 120(17), 8079–8088.

[26] Vidal-Henriquez, E., Zykov, V., Bodenschatz, E., et al., 2017. Convective instability and boundary driven oscillations in a reaction-diffusion-advection model. Chaos. 27(10), 103110.

[27] Shigesada, N., Kawasaki, K., Teramoto, E., 1979. Spatial segregation of interacting species. Journal of Theoretical Biology. 79(1), 83–99.

[28] Petrov, V., Scott, S.K., Showalter, K., 1994. Excitability, wave reflection, and wave splitting in a cubic autocatalysis reaction-diffusion system. Philosophical Transactions of the Royal Society A: Mathematical, Physical and Engineering Sciences. 347(1685), 631–642.

[29] Brindley, J., Biktashev, V., Tsyganov, M., 2005. Invasion waves in populations with excitable dynamics. Biological Invasions. 7(5), 807–816.

[30] Bate, A.M., Hilker, F.M., 2019. Prey-taxis and travelling waves in an eco-epidemiological model. Bulletin of Mathematical Biology. 81(4), 995–1030.

[31] Singh, A., Mandal, S., Tiwari, P.K., et al., 2025. Spatiotemporal dynamics of a modified Leslie-Gower predator-prey model: Effects of diffusion and taxis-driven movements on pattern formation. Nonlinear Analysis: Modelling and Control. 30(6), 1121–1144.

[32] Sun, Z., Jiang, W., 2024. Bifurcation and spatial patterns driven by predator-taxis in a predator-prey system with Beddington-DeAngelis functional response. Discrete and Continuous Dynamical Systems - B. 29(10), 4043–4070.

[33] Gao, X., 2022. Global solution and spatial patterns for a ratio-dependent predator-prey model with predator-taxis. Results in Mathematics. 77(2), 66.

[34] Kareiva, P., Odell, G., 1987. Swarms of predators exhibit ”prey-taxis” if individual predators use area-restricted search. The American Naturalist. 130, 233–270.

[35] Tyutyunov, Y.V., Titova, L.I., Senina, I.N., 2017. Prey-taxis destabilizes homogeneous stationary state in spatial Gause-Kolmogorov-type model for predator-prey system. Ecological Complexity. 31, 170–180.

[36] Grunbaum, D., 1998. Using spatially explicit models to characterize foraging performance in heterogeneous landscapes. The American Naturalist. 151, 97–113.

[37] Lee, J.M., Hillen, T., Lewis, M.A., 2008. Continuous traveling waves for prey-taxis. Bulletin of Mathematical Biology. 70, 654–676.

[38] Lee, J.M., Hillen, T., Lewis, M.A., 2009. Pattern formation in prey-taxis systems. Journal of Biological Dynamics. 3, 551–573.

[39] Ainseba, B.E., Bendahmane, M., Noussair, A., 2008. A reaction-diffusion system modeling predator-prey with prey-taxis. Nonlinear Analysis: Real World Applications. 9, 2086–2105.

[40] Sapoukhina, N., Tyutyunov, Y., Arditi, R., 2003. The role of prey taxis in biological control: A spatial theoretical model. The American Naturalist. 162, 61–76.

[41] Chakraborty, A., Singh, M., Lucy, D., et al., 2007. Predator-prey model with prey-taxis and diffusion. Mathematical and Computer Modelling. 46, 482–498.

[42] Chen, M., Wu, R., 2023. Steady-State Bifurcation in Previte-Hoffman Model. International Journal of Bifurcation and Chaos. 33(2), 2350020.

[43] Chen, M., Srivastava, H.M., 2023. Stability of bifurcating solution of a predator-prey model. Chaos, Solitons & Fractals. 168, 113153.

[44] Chen, M., Wu, R., 2023. Dynamics of a harvested predator-prey model with predator-taxis. Bulletin of the Malaysian Mathematical Sciences Society. 46(2), 76.

[45] Chen, M., Srivastava, H., 2023. Existence and stability of bifurcating solution of a chemotaxis model. Proceedings of the American Mathematical Society. 151(11), 4735–4749.

[46] Cosner, C., DeAngelis, D.L., Ault, J.S., et al., 1999. Effects of spatial grouping on the functional response of predators. Theoretical Population Biology. 56(1),

65–75.

[47] Li, S., Xiong, Z., Wang, X., 2010. The study of a predator-prey system with group defense and impulsive control strategy. Applied Mathematical Modelling. 34(9), 2546–2561.

[48] Berezovskaya, F.S., Song, B., Castillo-Chavez, C., 2010. Role of Prey Dispersal and Refuges on Predator-Prey Dynamics. SIAM Journal on Applied Mathematics. 70(6), 1821–1839.

[49] Murray, J.D., 2003. Mathematical Biology: II: Spatial Models and Biomedical Applications. Springer: New York, NY, USA.

[50] Cantrell, R.S., Cosner, C., 2004. Spatial Ecology via Reaction-Diffusion Equations. John Wiley & Sons: Hoboken, NJ, USA.

[51] Okubo, A., Levin, S.A., 2001. Diffusion and Ecological Problems: Modern Perspectives. Springer: New York, NY, USA.

[52] Freedman, H.I., 1980. Deterministic Mathematical Models in Population Ecology. Marcel Dekker, Inc.: New York, NY, USA. Available from: https://cir.nii.ac.jp/crid/1970586434821937342

[53] Hsu, S.B., Hwang, T.W., Kuang, Y., 2001. Global analysis of the Michaelis-Menten-type ratio-dependent predator-prey system. Journal of Mathematical Biology. 42(6), 489–506.

[54] Chattopadhyay, J., Arino, O., 1999. A predator-prey model with disease in the prey. Nonlinear Analysis: Theory, Methods & Applications. 36(6), 747–766.

[55] Perko, L., 2013. Differential Equations and Dynamical Systems. Springer Science & Business Media: Berlin, Germany.

[56] Hofbauer, J., Sigmund, K., 1998. Evolutionary Games and Population Dynamics. Cambridge University Press: Cambridge, UK.

[57] Morton, K.W., Mayers, D.F., 2005. Numerical Solution of Partial Differential Equations: An Introduction. Cambridge University Press: Cambridge, UK.

[58] LeVeque, R.J., 2007. Finite Difference Methods for Ordinary and Partial Differential Equations: Steady-State and Time-Dependent Problems. Society for Industrial and Applied Mathematics: Philadelphia, PA, USA.

[59] Smith, G.D., 1985. Numerical Solution of Partial Differential Equations: Finite Difference Methods. Oxford University Press: Oxford, UK.

[60] Roy, S., Sajan, Tiwari, P.K., et al., 2024. Dynamics of a stage-structured predator-prey system with fear-induced group defense in autonomous and nonautonomous settings. Chaos: An Interdisciplinary Journal of Nonlinear Science. 34(6), 063133.